Adaptive Time-Switching Based Energy Harvesting Relaying Protocols

Haiyang Ding, *Member*, *IEEE*, Xiaodong Wang, Daniel Benevides da Costa, *Senior Member*, *IEEE*, Yunfei Chen, *Senior Member*, *IEEE*, and Fengkui Gong

Abstract

Considering a dual-hop energy-harvesting (EH) relaying system, this paper advocates novel relaying protocols based on adaptive time-switching (TS) for amplify-and-forward and decode-and-forward modes, respectively. The optimal TS factor is first studied, which is adaptively adjusted based on the dual-hop channel state information (CSI), accumulated energy and threshold signal-to-noise ratio (SNR), to achieve the maximum throughput efficiency per block. To reduce the CSI overhead at the EH relay, low-complexity TS factor design is presented which only needs single-hop CSI to determine the TS factor. Theoretical results show that, in comparison with the conventional solutions, the proposed optimal/low-complexity TS factor can achieve higher limiting throughput efficiency for sufficiently small threshold SNR. As the threshold SNR approaches infinity, the throughput efficiency of the proposed optimal/low-complexity TS factor tends to zero in a much slower pace than that of the conventional solutions. Simulation results are presented to corroborate the proposed methodology.

Index Terms

Energy transfer, relay, time-switching, throughput efficiency, wireless energy harvesting.

H. Ding is with the State Key Laboratory of Integrated Service Networks, Xidian University, Xi'an, China and with Xi'an Communication Institute, Xi'an, China. His work is supported by the Natural Science Foundation of Shaanxi province (Grant No. S2014JC13058), by the National Natural Science Foundation of China (Grant No. 61301135) and by the open research fund of the State Key Lab. of ISN under grant ISN15-05 (email: dinghy2003@hotmail.com).

X. Wang is with the Department of Electrical Engineering, Columbia University, NY, USA (email: wangx@ee.columbia.edu).

D. B. da Costa is with the Department of Computer Engineering, Federal University of Ceará, Sobral, CE, Brazil (email: danielbcosta@ieee.org). The work is supported by the CNPq (Grant No. 304301/2014-0.)

Y. Chen is with the School of Engineering, University of Warwick, Coventry, U.K. CV4 7AL (e-mail: Yunfei.Chen@warwick.ac.uk).

Fengkui Gong is with the State Key Laboratory of Integrated Service Networks, Xidian University, Xi'an 710071, China (e-mail: fkgong@xidian.edu.cn).

I. Introduction

In the late 19th century, Nikola Tesla experimentally demonstrated wireless energy transfer (WET). After that, in the majority of the subsequent developments of wireless communications techniques, the emphasis was placed on information transmission instead of energy transfer. Until recently, the seminal work of [1] shed some light on the importance of wireless energy/power transfer in wireless communications systems. In particular, simultaneous wireless information and power transfer (SWIPT) was highlighted [2]. Since then, the rate-energy tradeoff has been investigated considering various point-to-point network setups, such as single-input-single-output (SISO) [3]–[5], single-input-multiple-output (SIMO) [6], multiple-input-single-output (MISO) [7], and multiple-input-multiple-output (MIMO) [8], [9]. To make SWIPT feasible in realistic communications systems, [3] designed two novel receiver architectures, namely, the time-switching (TS) based and power-splitting (PS) based receivers and investigated their rate-energy tradeoffs. Focusing on the PS architecture, [6] proposed a dynamic PS approach which can split the received signal into two streams with adjustable power levels for information decoding and energy harvesting separately based on the instantaneous channel condition.

In addition to the aforementioned point-to-point network setups, the concept of SWIPT has also been extended to cooperative diversity systems. In this regard, based on the TS and PS receiver architectures, [10] designed two amplify-and-forward (AF) relaying protocols and analyzed their throughput performance. Making use of a PS-based energy-harvesting (EH) receiver architecture, [11] studied the power allocation strategies at the EH relay to assist the information transmission among multiple source-destination pairs. In [12], by using a stochastic geometry tool, the authors investigated the performance of a network with a random number of transmitter-receiver pairs, where the PS-based receiver architecture was employed. By taking the spatial randomness of user locations into account, the authors of [13] characterized the system outage probability of an EH relay system with multiple source-destination pairs. In [14], a three-node cooperative network with an EH relay was studied and a fundamental switching between EH and data relaying was introduced. In [15], the authors investigated a relay network where source and relay harvest energy from the access-point during the downlink phase and cooperate during the uplink phase,

and then proposed a harvest-then-cooperate protocol based on the TS-based EH receiver. In [16], by modeling the charging/discharging behavior of the battery as a two-state Markov chain (fully charged or empty), the author investigated the outage performance of several relay selection schemes. For a multi-relay cooperative network, [17] assumed that each EH relay may operate in EH mode or in information forwarding mode during each transmission block, where each transmission block is composed of two time slots with fixed length and the first time slot is used to harvest energy in EH mode. Reference [18] proposed a relay selection scheme considering both channel state information (CSI) and battery status of EH relays, where the transmit power at relay is fixed and identical for all EH relays. In [19], a distributed PS framework using game theory was developed, which was then extended to the more general network setting. Very recently, in order to allow energy accumulation at the EH relay, [20] designed several TS-based EH relaying protocols, where the energy constrained relay continues to harvest energy from the radio-frequency (RF) signal transmitted by the source until it has harvested adequate energy to transmit the source's information with a fixed preset transmit power. Particularly, it was shown in [20] that the proposed protocols outperform the existing fixed-time duration EH protocols owing to the online switching between EH and information transmission (IT).

Even though the proposed protocols in [20] dynamically adjust the time duration of EH operation at the relay to support a TS-based IT, the system throughput efficiency cannot be effectively guaranteed due to the random fluctuation of wireless fading channels. Specifically, the fixed transmit-power setting at the relay cannot avoid the information outage when the second-hop channel is in deep fading. Motivated by this, in this paper we aim to design robust EH relaying protocols with adaptive TS factor and transmit power setting at the EH relay, which can achieve a superior throughput efficiency compared with the conventional solutions. The main contributions of this work can be summarized as below:

i) Considering continuous-time EH, we propose two TS-based EH relaying protocols for AF and decode-and-forward (DF) modes, respectively. Our results show that the TS factor and the transmission power at the relay should be jointly designed to achieve an optimal throughput efficiency, and that optimizing the TS factor alone is inadequate as performed in the literature.

ii) Representative numerical examples are shown to illustrate the superior performance[1] of the proposed optimal TS factor setting over conventional ones. For both AF and DF modes under typical operation conditions, to achieve a throughput efficiency of 0.4, the proposed optimal TS factor design can provide more than 8.6 dB threshold signal-to-noise ratio (SNR) gain[2] over the conventional solutions, whereas to attain a throughput efficiency of 0.3, the proposed protocols promise a threshold SNR gain of more than 5.8 dB over the conventional ones.

iii) To reduce the CSI overhead at EH relay, we further present low-complexity TS factor design for AF and DF modes, respectively. To gain insights into the performance difference between the proposed protocols and the prior ones, it is important to capture the scaling law of the throughput efficiency. For such, by invoking an asymptotic analysis based on the inequality $(x+1)^{-1}e^{-x} < E_1(x)$ [23, Eq. (5.1.19)], we are able to disclose the scaling law of the throughput efficiency for the conventional protocols as well as the proposed ones. Theoretical analysis reveals that for a sufficiently low threshold SNR, both the optimal and the low-complexity TS factor setting can achieve a limiting throughput efficiency of 0.5, whereas the counterpart of the conventional solutions is less than 0.5. On the other hand, as the threshold SNR goes to infinity, the throughput efficiency of both the optimal and the low-complexity TS factor setting approaches to zero in a much slower pace than that of the conventional solutions.

II. System Model and Proposed EH Relaying Protocols

In this section, for both AF and DF relaying modes, we first present the system model and the conventional EH protocols, based on which the proposed EH protocols are introduced. For both AF and DF relaying modes, the information transmission is organized into blocks and each block has a time duration of T seconds. In addition, slow fading channels are assumed such that the channel coefficients remain constant during one block.

[1]Owing to the remarkable performance advantage, the proposed optimal TS factor setting can tolerate a higher threshold SNR requirement at the destination to achieve the same throughput efficiency with the conventional protocol. In addition, the proposed low-complexity TS factor setting serves as a beneficial supplement to the optimal TS factor setting to achieve the limiting throughput performance for sufficiently small threshold SNR. This allows the proposed protocols to tolerate a tougher threshold SNR requirement to achieve excellent throughput performance, leading to potential applications in transmission reliability-critical EH relaying scenarios.

[2]To achieve the same throughput efficiency, a good TS factor setting can tolerate a higher threshold SNR requirement. Hereafter, we refer to this additional threshold SNR margin as threshold SNR gain.

A. AF Relaying

Herein, we first present the system model for the TS-based AF relaying. Then, we introduce the conventional TS-based AF relaying protocol, inspired by which we propose our new adaptive TS-based AF relaying protocol.

1) System Model: For AF relaying, the received signal at the relay node can be expressed as

$$y_{r,i} = \sqrt{P_s d_1^{-m}} h_i s_i + n_{r,i}, \tag{1}$$

where i denotes the block index, d_1 is the distance between source (S) and relay (R), m is the path loss exponent, P_s denotes the transmit power at source, h_i represents the Rayleigh[3] faded channel coefficient of the first-hop link $S \to R$, s_i denotes the normalized signal from source, $n_{r,i}$ indicates the additive white Gaussian noise (AWGN) at the relay node with variance $\sigma_{n_r}^2$.

For each block, the AF relay first harvests energy from the source such that during IT time it could forward the received signal to the destination with transmit power P_r. Specifically, the transmitted signal at the EH relay is given as

$$x_{r,i} = \frac{\sqrt{P_r} y_{r,i}}{\sqrt{P_s |h_i|^2 d_1^{-m} + \sigma_{n_r}^2}}. \tag{2}$$

Then, the received signal at the destination can be written as

$$y_{d,i} = g_i \sqrt{d_2^{-m}} x_{r,i} + n_{d,i} = \frac{\sqrt{P_r P_s d_2^{-m}} h_i g_i s_i}{\sqrt{P_s |h_i|^2 + d_1^m \sigma_{n_r}^2}} + \frac{\sqrt{P_r d_2^{-m} d_1^m} g_i n_{r,i}}{\sqrt{P_s |h_i|^2 + d_1^m \sigma_{n_r}^2}} + n_{d,i}, \tag{3}$$

in which d_2 denotes the distance between relay (R) and destination (D), g_i is the Rayleigh faded channel coefficient of the second-hop link $R \to D$, and $n_{d,i}$ is the AWGN at the destination with variance $\sigma_{n_d}^2$. Therefore, the received SNR at the destination can be written as

$$\gamma_{d,i} = \frac{P_s P_r |h_i|^2 |g_i|^2}{P_r |g_i|^2 d_1^m \sigma_{n_r}^2 + d_2^m \sigma_{n_d}^2 (P_s |h_i|^2 + d_1^m \sigma_{n_r}^2)} = \frac{\gamma_{sr,i} \gamma_{rd,i}}{\gamma_{sr,i} + \gamma_{rd,i} + 1}, \tag{4}$$

where $\gamma_{sr,i} \triangleq P_s |h_i|^2 / (d_1^m \sigma_{n_r}^2)$ and $\gamma_{rd,i} \triangleq P_r |g_i|^2 / (d_2^m \sigma_{n_d}^2)$. Note that the i-th block will suffer

[3]It is noteworthy that Rician fading can also be assumed for the first-hop link to incorporate the effects of LOS path component, which is an interesting topic for further study. Nonetheless, the Rician fading assumption would not change the limiting throughput performance of the proposed protocols for sufficiently small threshold SNR, as manifested by the ensuing theoretical results.

from outage if the received SNR at D falls below a given threshold SNR γ_0. As a result, the outage indicator can be defined as

$$I_{o,i} = \mathrm{I}(\gamma_{d,i} < \gamma_0), \tag{5}$$

where $\mathrm{I}(\cdot)$ equals to 1 if its argument is true and equals to 0 otherwise, as in [20].

2) Conventional TS-based AF Relaying Protocol: For each block, the EH operation takes up the first $\alpha_i T$ seconds, where α_i denotes the TS factor belonging to [0,1]. As such, the newly harvested energy within the i-th block is $\alpha_i T(\eta P_s |h_i|^2 / d_1^m)$, where η denotes the energy conversion efficiency[4]. During IT time, half of the time $\frac{(1-\alpha_i)T}{2}$ is used for $S \to R$ IT, and the remaining half time is used for $R \to D$ IT. In this protocol, the relay only harvests that much energy within each block that is required for its relaying transmission [20, Sect. III-B] such that at the end of each block the remaining energy will be zero. Since all of the harvested energy during EH time will be consumed during IT time, it is ready to determine the TS factor α_i as [20, Eq. (8)]

$$\alpha_i = \frac{d_1^m P_r}{2\eta P_s |h_i|^2 + d_1^m P_r}. \tag{6}$$

Based on (5) and (6), the throughput efficiency of the i-th block can be written as

$$\tau_i = \frac{(1 - I_{o,i})(1 - \alpha_i)}{2}. \tag{7}$$

Although the TS factor setting in (6) guarantees that all the harvested energy during the EH time is utilized to support IT, it follows from (7) that such a TS factor setting can not boost the throughput efficiency. This is because the TS factor in (6) is based on a constant transmit-power setting at relay (P_r) which cannot effectively reduce the outage events as defined in (5). This motivates us to design a robust TS-based AF relaying protocol.

[4]The energy conversion efficiency η can be considered as an equivalent energy conversion efficiency which is a product of two quantities, i.e., $\eta = \zeta\tilde{\eta}$. Herein, $\tilde{\eta}$ denotes the energy conversion efficiency of the RF-to-DC circuit, and ζ represents the proportion of the harvested energy which is used for the transmit power at EH relay. This equivalent energy conversion efficiency is applicable to both AF and DF modes.

3) Proposed TS-based AF Relaying Protocol: For a given threshold γ_0, to avoid the information outage, it is required that $\gamma_{d,i} \geq \gamma_0$, which in turn leads to

$$(\gamma_{sr,i} - \gamma_0)\gamma_{rd,i} \geq \gamma_0(\gamma_{sr,i} + 1), \tag{8}$$

which means that for $\gamma_{sr,i} < \gamma_0$, (8) becomes an impossible event (i.e., information outage definitely happens[5]), whereas for $\gamma_{sr,i} \geq \gamma_0$, we have $P_r \geq d_2^m \sigma_{n_d}^2 \gamma_0(\gamma_{sr,i}+1)/(|g_i|^2(\gamma_{sr,i}-\gamma_0))$. Inspired by this, the transmit power of the EH relay can be determined as

$$\bar{P}_r \triangleq \max\left[0, \frac{d_2^m \sigma_{n_d}^2 \gamma_0(\gamma_{sr,i}+1)}{|g_i|^2(\gamma_{sr,i}-\gamma_0)}\right]. \tag{9}$$

Therefore, if the transmit power P_r at the EH relay is set to $\bar{P}_r$, the information outage will not happen between source and destination, provided that $\gamma_{sr,i} \geq \gamma_0$. Note that if the transmit power P_r at EH relay is further increased over $\bar{P}_r$, the available time proportion for IT $(1-\alpha_i)$ will be reduced such that the block-wise throughput efficiency will decrease accordingly. Consequently, with respect to the block-wise throughput efficiency, $\bar{P}_r$ is actually the optimal transmit power at the EH relay. All the harvested energy will be consumed for the ensuing IT in the current block such that the optimal TS factor α_i can be written as

$$\alpha_i = \frac{d_1^m \bar{P}_r}{2\eta P_s |h_i|^2 + d_1^m \bar{P}_r} \triangleq \ddot{\alpha}_i, \tag{10}$$

where $\bar{P}_r$ is given in (9). Then, the newly harvested energy within the i-th block is $\ddot{\alpha}_i T(\eta P_s |h_i|^2/d_1^m)$, while at the end of the i-th block, no energy remains.

Remark 1: With regard to the CSI requirement, the conventional TS factor setting in (6) requires the EH relay to keep track of the first-hop CSI $|h_i|^2$. In addition to the first-hop CSI, our proposal also requires the EH relay to keep track of the second-hop channel to calculate the TS factor and the transmit power at EH relay. To achieve this, the overhearing of the clear-to-send (CTS) packet from the destination can be invoked at the EH relay, as in [21]. It is noteworthy that this additional CSI requirement at relay is worthwhile and will significantly improve the

[5]To make a fair/straightforward comparison with the conventional TS-based AF relaying protocol, it is assumed that the AF relay keeps idle/silent in the current block, provided that $\gamma_{sr,i} < \gamma_0$.

throughput efficiency as shown by the numerical results in Section V.

For the proposed TS-based AF relaying protocol, the throughput efficiency of the i-th block can be written as

$$\tau_i = \frac{(1 - I_{o,i})(1 - \ddot{\alpha}_i)}{2}. \tag{11}$$

B. DF Relaying

In this part, we first present the system model for TS-based DF relaying. Then, we describe the conventional TS-based DF relaying protocol. Finally, we introduce a new TS-based DF relaying protocol.

1) System Model: For DF relaying, the received signal at the relay node is still given by (1). During IT time of the i-th block, the received signal at the destination can be expressed as

$$y_{d,i} = \sqrt{P_r d_2^{-m}} g_i s_i + n_{d,i}. \tag{12}$$

Then, based on (1) and (12), the SNR at relay and destination are given by

$$\gamma_{r,i} = \frac{P_s |h_i|^2}{d_1^m \sigma_{n_r}^2}, \quad \gamma_{d,i} = \frac{P_r |g_i|^2}{d_2^m \sigma_{n_d}^2}. \tag{13}$$

As a result, the outage indicator of the i-th block[6] can be written as in (5) with $\gamma_{d,i}$ given by (13).

2) Conventional TS-based DF Relaying Protocol: In this protocol, similar to AF mode, the EH relay merely harvests that much energy within each block that is required for IT. In the case of information outage at the relay node (i.e., $\gamma_{r,i} < \gamma_0$), the whole block will be dedicated to EH. Accordingly, three types of EH-IT pattern are possible for the conventional TS-based DF relaying protocol [20, Sect. IV.B].

a) The first type contains only a single EH-IT block, similar to the AF mode. For the single EH-IT block, by denoting the available harvested energy at the start of the i-th block as $E_i(0)$,

[6]As stated in [20], the case $\gamma_{r,i} < \gamma_0$ is not part of the outage indicator for DF relaying, since the whole block will be in EH mode instead of IT mode in this case. In addition, the TS factor setting defined afterwards guarantees that the throughput efficiency of the current block will be zero under such scenarios.

we have $E_i(0) < P_r T/2$ and the first portion of the block time $\alpha_i T$ is used to EH, while the remaining portion of the block time $(1-\alpha_i)T$ within the i-th block is utilized for IT.

b) The second type contains n consecutive EH blocks due to relay outage, before an EH-IT block. In this case, the energy is accumulated during the EH blocks and only reaches the required level sometime during the EH-IT block. Within the EH-IT block, the accumulated energy is then consumed for IT such that the initial energy of the next pattern equals to zero, i.e., $E_o = 0$.

c) The third type contains n consecutive EH blocks due to relay outage, before an IT block. In this case, the energy is accumulated during the EH blocks and exceeds the required level for IT. As a result, this type of EH-IT pattern is composed of n EH blocks followed by an IT block, and the initial energy of the next EH-IT pattern satisfies to $E_o > 0$.

Consequently, the accumulated energy at the time instant $\alpha_i T$ during the i-th EH-IT block is given by

$$E_i(\alpha_i T) = \frac{\eta P_s |h_i|^2}{d_1^m} \alpha_i T + E_i(0). \tag{14}$$

Then, the TS factor α_i and $E_i(T)$ for the i-th block can be determined as

$$\alpha_i = \begin{cases} \frac{d_1^m P_r T - 2E_i(0) d_1^m}{2\eta P_s |h_i|^2 T + d_1^m P_r T}, \ \text{if} \ |h_i|^2 \geq \bar{a}, \ E_i(0) \leq \frac{P_r T}{2}, \\ 0, \ \text{if} \ |h_i|^2 \geq \bar{a}, \ E_i(0) > \frac{P_r T}{2}, \\ 1, \ \text{if} \ |h_i|^2 < \bar{a}, \end{cases} \tag{15}$$

$$E_i(T) = \begin{cases} 0, \ \text{if} \ 0 < \alpha_i < 1, \\ E_i(0) + \frac{\eta P_s |h_i|^2 T}{d_1^m}, \ \text{if} \ \alpha_i = 1, \\ E_i(0) - \frac{P_r T}{2}, \ \text{if} \ \alpha_i = 0, \end{cases} \tag{16}$$

in which $\bar{a} \triangleq \frac{\gamma_0 d_1^m \sigma_{nr}^2}{P_s}$. Therefore, the throughput efficiency of the i-th block can be expressed as

$$\tau_i = \frac{(1 - I_{o,i})(1 - \alpha_i)}{2}, \tag{17}$$

where α_i and $I_{o,i}$ are defined, respectively, as in (15) and (5), with $\gamma_{d,i}$ given by (13).

Notably, for the conventional TS-based DF relaying protocol, neither the TS factor setting in (15) nor the constant transmit-power P_r at relay takes into account of the second-hop fading channel (i.e., g_i), which leads to a high-risk second-hop information transmission. Thus, it follows from (17) that the throughput efficiency can not be effectively guaranteed. This inspires us to design a robust TS-based DF relaying protocol.

3) Proposed TS-based DF Relaying Protocol: To guarantee that the second-hop link does not suffer from information outage, the following inequality must hold

$$P_r \geq \frac{d_2^m \sigma_{n_d}^2 \gamma_0}{|g_i|^2} \triangleq \bar{P}_r. \tag{18}$$

Remark 2: As shown in (18), the EH relay needs the second-hop CSI. This additional CSI overhead will be well paid off in the form of a remarkable throughput enhancement. In addition, the second-hop CSI can be acquired by the EH relay in the same way as in the AF mode [21], [22].

Accordingly, the TS factor of the proposed TS-based DF relaying protocol can be expressed as

$$\alpha_i \triangleq \breve{\alpha}_i = \begin{cases} \frac{d_1^m \bar{P}_r T - 2E_i(0) d_1^m}{2\eta P_s |h_i|^2 T + d_1^m P_r T}, & \text{if } |h_i|^2 \geq \bar{a},\ E_i(0) \leq \frac{\bar{P}_r T}{2}, \\ 0, & \text{if } |h_i|^2 \geq \bar{a},\ E_i(0) > \frac{\bar{P}_r T}{2}, \\ 1, & \text{if } |h_i|^2 < \bar{a}. \end{cases} \tag{19}$$

It follows from (19) that the newly harvested energy within the i-th block is $\breve{\alpha}_i T(\eta P_s |h_i|^2 / d_1^m)$. Therefore, at the end of the i-th block, the remaining energy can be written as

$$E_i(T) = \begin{cases} 0, & \text{if } 0 < \breve{\alpha}_i < 1, \\ E_i(0) + \frac{\eta P_s |h_i|^2 T}{d_1^m}, & \text{if } \breve{\alpha}_i = 1, \\ E_i(0) - \frac{\bar{P}_r T}{2}, & \text{if } \breve{\alpha}_i = 0. \end{cases} \tag{20}$$

Finally, for the proposed TS-based DF relaying protocol, the throughput efficiency of the i-th block can be formulated as

$$\tau_i = \frac{(1 - I_{o,i})(1 - \breve{\alpha}_i)}{2}. \tag{21}$$

III. Throughput Analysis

A. AF Relaying

Proposition 1: The throughput efficiency of the proposed TS-based AF relaying protocol with continuous-time EH can be derived as

$$\tau = \frac{1}{2}e^{-\bar{a}} - \frac{1}{2}\xi, \tag{22}$$

where ξ is given by

$$\xi = \int_0^\infty \varpi(z) e^{\varpi(z)-(z+\bar{a})} E_1(\varpi(z)) dz, \tag{23}$$

in which[7] $\varpi(z) = \frac{d_1^m d_2^m \sigma_{n_d}^2 \gamma_0}{2\eta P_s \bar{a}} \left(z + \bar{a} + \frac{\bar{a}}{\gamma_0}\right) \left(\frac{1}{z} - \frac{1}{z+\bar{a}}\right)$. In addition, a tight upper bound of the throughput efficiency can be written as

$$\tau^{\text{UB}} = \frac{1}{2}e^{-\bar{a}} - \frac{1}{2}\xi^{\text{LB}}, \tag{24}$$

where ξ^{LB} is given by

$$\xi^{\text{LB}} = \int_0^\infty \frac{\varpi(z)}{\varpi(z)+1} e^{-(z+\bar{a})} dz. \tag{25}$$

Proof: Please refer to Appendix A. ■

Corollary 1: For the proposed TS-based AF relaying protocol with continuous-time EH, the throughput efficiency can be approximately expressed as

$$\tau \approx \frac{1}{2}e^{-\bar{a}} - \frac{1}{2} D_0 e^{-\bar{a}+D_0} E_1(D_0). \tag{26a}$$

where $D_0 \triangleq \frac{d_1^m d_2^m \sigma_{n_d}^2 \gamma_0}{2\eta P_s}$. Then, a simplified approximation to (26a) can be written as

$$\tau \approx \frac{1}{2} \frac{e^{-\bar{a}}}{D_0 + 1}. \tag{26b}$$

It follows from (26b) that as $\gamma_0 \to 0$, the throughput efficiency approaches to 0.5, whereas as

[7]Throughout this paper, we use $E_1(x)$ to denote the exponential integral function [23, Eq. (5.1.1)], and employ the notation $E_i(t)$ with $t \in [0, T]$ to represent the remaining energy at instant t of the i-th block.

$\gamma_0 \to \infty$, the throughput efficiency scales as

$$\tau \approx \frac{\eta P_s}{d_1^m d_2^m \sigma_{n_d}^2} \frac{1}{\gamma_0} e^{-\bar{a}} \propto \frac{1}{\gamma_0} e^{-\frac{d_1^m \sigma_{n_r}^2 \gamma_0}{P_s}}. \tag{27}$$

Proof: Please refer to Appendix B.1. ■

Corollary 2: For the conventional TS-based AF relaying protocol with continuous-time EH, as $\gamma_0 \to 0$, the throughput efficiency can be approximated as

$$\tau \approx \frac{1}{2} \left(1 - c d_1^m P_r v\right), \tag{28}$$

where $v = \int_0^\infty \frac{e^{-x - \frac{ad+bc}{c^2 x}}}{2c\eta P_s x + 2\eta P_s d + c d_1^m P_r} dx$, with $a = P_s d_2^m \sigma_{n_d}^2 \gamma_0$, $b = d_1^m d_2^m \sigma_{n_r}^2 \sigma_{n_d}^2 \gamma_0$, $c = P_s P_r$, and $d = P_r d_1^m \sigma_{n_r}^2 \gamma_0$. On the other hand, as $\gamma_0 \to \infty$, the throughput efficiency can be approximately written as

$$\tau \approx \sqrt{\frac{\pi}{8}} u^{\frac{1}{2}} e^{-\left(\sqrt{\bar{a}} + \sqrt{\bar{b}}\right)^2}, \tag{29}$$

where $\bar{a}$ is the same as before, $u = \sqrt{\frac{4(ad+bc)}{c^2}}$, and $\bar{b} \triangleq \gamma_0 d_2^m \sigma_{n_d}^2 / P_r$.

Proof: Please refer to Appendix B.2. ■

Remark 3: It follows from (26b) of Corollary 1 that as $\gamma_0 \to 0$, the throughput efficiency of the proposed TS-based AF relaying protocol approaches to 0.5, which is the limiting throughput efficiency for half-duplex relaying. In contrast, Corollary 2 manifests that as $\gamma_0 \to 0$, the throughput efficiency of the conventional protocol is less than 0.5. On the other hand, it follows from Corollary 1 that as $\gamma_0 \to \infty$, the throughput efficiency of the proposed protocol scales as $\frac{1}{\gamma_0} e^{-\bar{a}}$. Whereas for the conventional TS-based AF relaying protocol, the scaling law of throughput efficiency obeys the law of $\sqrt{\gamma_0} e^{-\left(\sqrt{\bar{a}} + \sqrt{\bar{b}}\right)^2}$, a much higher decaying rate than the proposed protocol. The above limiting performance demonstrates the advantage of the proposed adaptive TS factor setting.

Next, we present a pair of tight bounds for the throughput efficiency, which is summarized in the following proposition.

Proposition 2: For the proposed TS-based AF relaying protocol with continuous-time EH, a

pair of tight lower/upper bounds of the throughput efficiency can be formulated as

$$\hat{\tau}^{\mathrm{LB}} = \frac{1}{2}e^{-\bar{a}} - \frac{1}{2}\tilde{\xi}^{\mathrm{UB}}, \tag{30}$$

$$\hat{\tau}^{\mathrm{UB}} = \frac{1}{2}e^{-\bar{a}} - \frac{1}{2}\tilde{\xi}^{\mathrm{LB}}, \tag{31}$$

in which $\tilde{\xi}^{\mathrm{LB}}$ and $\tilde{\xi}^{\mathrm{UB}}$ can be expressed as

$$\tilde{\xi}^{\mathrm{LB}} = \frac{d_2^m \sigma_{n_d}^2 e^{-\bar{a}}}{4\eta\sigma_{n_r}^2} \int_0^\infty \frac{\bar{a}z + \bar{a}^2(1+\gamma_0^{-1})}{z(z+\bar{a})} e^{-z} \ln\left(1 + \frac{4\eta\sigma_{n_r}^2 z(z+\bar{a})}{d_2^m \sigma_{n_d}^2 [\bar{a}z + \bar{a}^2(1+\gamma_0^{-1})]}\right) dz, \tag{32}$$

$$\tilde{\xi}^{\mathrm{UB}} = \frac{d_2^m \sigma_{n_d}^2 e^{-\bar{a}}}{2\eta\sigma_{n_r}^2} \int_0^\infty \frac{\bar{a}z + \bar{a}^2(1+\gamma_0^{-1})}{z(z+\bar{a})} e^{-z} \ln\left(1 + \frac{2\eta\sigma_{n_r}^2 z(z+\bar{a})}{d_2^m \sigma_{n_d}^2 [\bar{a}z + \bar{a}^2(1+\gamma_0^{-1})]}\right) dz. \tag{33}$$

Proof: Making use of the inequalities for the exponential integral function $E_1(\cdot)$ [23, Eq. (5.1.20)], we can arrive at the lower and upper bounds for the variate ξ in (23), as shown by (32) and (33). This in turn leads to the throughput bounds given by (30) and (31).

Remark 4: Note that in comparison with (25), the integrands of (32) and (33) are more complicated, which however can yield tighter throughput bounds. In addition, the integrands in (32) and (33) are merely composed of elementary functions, e.g., exponentials and logarithms, which are easy to calculate numerically.

B. DF Relaying

In this subsection, we first present a tight bound for the throughput efficiency of the conventional TS-based DF relaying protocol with continuous-time EH. Based on this bound, we characterize the throughput efficiency of the proposed TS-based DF relaying protocol.

Proposition 3: For the conventional TS-based DF relaying protocol with continuous-time EH, a tight lower bound of the throughput efficiency can be written as

$$\tau^{\mathrm{LB}} = \frac{e^{-\bar{a}-\bar{b}}}{2}(I_0 + I_1 + I_2), \tag{34}$$

where I_0, I_1, and I_2 can be expressed, respectively, as

$$I_0 = e^{-\bar{a}} - \frac{d_1^m P_r}{2\eta P_s} e^{\frac{d_1^m P_r}{2\eta P_s}} E_1\left(\bar{a} + \frac{d_1^m P_r}{2\eta P_s}\right), \tag{35a}$$

$$I_1 = e^{-\bar{a}}(1 - e^{-\bar{a}}) - \frac{e^{\frac{d_1^m P_r}{2\eta P_s}}}{2\eta P_s} E_1\left(\bar{a} + \frac{d_1^m P_r}{2\eta P_s}\right)\left[d_1^m P_r\left(1 - e^{-q_1}\right) - 2\eta P_s(1 - e^{-q_1}(1 + q_1))\right], \tag{35b}$$

$$I_2 = \begin{cases} e^{-\bar{a}}(1 - e^{-\bar{a}})^2 - \frac{e^{\frac{d_1^m P_r}{2\eta P_s}} E_1\left(\bar{a} + \frac{d_1^m P_r}{2\eta P_s}\right)}{2\eta P_s}\{d_1^m P_r \varphi_1 - 2\eta P_s \varphi_2\}, & \text{if } \bar{a} \leq \frac{d_1^m P_r}{2\eta P_s}, \\ e^{-\bar{a}}(1 - e^{-\bar{a}})^2 - \frac{e^{\frac{d_1^m P_r}{2\eta P_s}} E_1\left(\bar{a} + \frac{d_1^m P_r}{2\eta P_s}\right)}{2\eta P_s}\{d_1^m P_r \varphi_3 - 2\eta P_s \varphi_4\}, & \text{if } \bar{a} > \frac{d_1^m P_r}{2\eta P_s}, \end{cases} \tag{35c}$$

where the variates φ_1, φ_2, φ_3, and φ_4 are given, respectively, by

$$\varphi_1 = 1 - 2e^{-\bar{a}} + [1 - 2(\bar{a} - q_2)]e^{-2q_2}, \tag{36a}$$

$$\varphi_2 = 2 + e^{-\bar{a}}(-4 - 2\bar{a}) + e^{-2q_2}[2 + 2q_2 - 2(1 + 2q_2)(\bar{a} - q_2)], \tag{36b}$$

$$\varphi_3 = 1 - (1 + 2q_2)e^{-2q_2}, \tag{36c}$$

$$\varphi_4 = 2 - 2e^{-2q_2}(1 + 2q_2 + 2q_2^2), \tag{36d}$$

in which we have $q_1 \triangleq \min\left[\bar{a}, \frac{d_1^m P_r}{2\eta P_s}\right]$ and $q_2 \triangleq \min\left[\bar{a}, \frac{d_1^m P_r}{4\eta P_s}\right]$.

Proof: Please refer to Appendix C. ■

Corollary 3: For the conventional TS-based DF relaying protocol with continuous-time EH, as $\gamma_0 \to 0$, the throughput efficiency can be approximately written as

$$\tau \approx \frac{1}{2}\left(1 - \frac{d_1^m P_r}{2\eta P_s} e^{\frac{d_1^m P_r}{2\eta P_s}} E_1\left(\frac{d_1^m P_r}{2\eta P_s}\right)\right). \tag{37}$$

Whereas as $\gamma_0 \to \infty$, the throughput efficiency can be approximately expressed as

$$\tau \approx \frac{3}{2} e^{-(C_1 + C_2)\gamma_0} \propto e^{-(C_1 + C_2)\gamma_0} \to 0, \tag{38}$$

where $C_1 \triangleq \frac{2\bar{a}}{\gamma_0} = \frac{2d_1^m \sigma_{nr}^2}{P_s}$ and $C_2 \triangleq \frac{\bar{b}}{\gamma_0} = \frac{d_2^m \sigma_{n_d}^2}{P_r}$.

Proof: Please refer to Appendix D. ■

Remark 5:

(i) It follows from Corollary 3 that for a constant transmit power P_r [20], as $\gamma_0 \to 0$, we have $\bar{a} \to 0$ and $\bar{b} \to 0$ such that the throughput efficiency approaches (37), which is less than 0.5.

(ii) As $\gamma_0 \to \infty$, it follows from (38) that the throughput efficiency tends to zero with a scaling law of $e^{-(C_1+C_2)\gamma_0}$.

Similar to the AF relaying, the lack of the second-hop CSI knowledge in the setting of TS factor and relay's transmit power cannot guarantee a reliable dual-hop transmission. In contrast, by monitoring the second-hop CSI, our proposal could cut down the information outage, improving therefore the throughput performance. In the following, the throughput efficiency of the proposed TS-based DF relaying protocol will be characterized.

Proposition 4: For the proposed TS-based DF relaying protocol with continuous-time EH, a tight lower bound of the throughput efficiency can be written as

$$\hat{\tau}^{\mathrm{LB}} = \frac{e^{-\bar{a}}}{2}(\breve{I}_0 + \breve{I}_1 + \breve{I}_2), \tag{39}$$

where $\breve{I}_0$, $\breve{I}_1$, and $\breve{I}_2$ are given, respectively, by

$$\breve{I}_0 = e^{-\bar{a}} - f_1(0,\infty), \tag{40a}$$

$$\breve{I}_1 = e^{-\bar{a}}(1-e^{-\bar{a}}) - f_1(0,\infty) + e^{-\bar{a}} f_1(0,2\theta_0) + f_3(0,\infty) - e^{-\bar{a}}(1+\bar{a}) f_3(0,2\theta_0) - f_4(2\theta_0,\infty), \tag{40b}$$

$$\begin{aligned}\breve{I}_2 = {} & e^{-\bar{a}}\varphi_1^{(1)}(1-e^{-\theta_0}) - \varphi_2^{(1)} f_1(0,\theta_0) + \varphi_3^{(1)} f_3(0,\theta_0) + e^{-\bar{a}}\varphi_1^{(2)}(e^{-\theta_0} - e^{-2\theta_0}) \\ & - (1-2e^{-\bar{a}}) f_1(\theta_0,2\theta_0) + f_2(\theta_0,2\theta_0) + [2 - 2e^{-\bar{a}}(2+\bar{a})] f_3(\theta_0,2\theta_0) + 2(1-\bar{a}) f_4(\theta_0,2\theta_0) \\ & + e^{-2\theta_0-\bar{a}}(1-e^{-\bar{a}})^2 - f_1(2\theta_0,\infty) - f_2(2\theta_0,\infty) + 2f_3(2\theta_0,\infty) - 2f_4(2\theta_0,\infty),\end{aligned} \tag{40c}$$

in which we have

$$f_1(a,b)=\int_a^b \frac{\omega_1}{x}e^{-x+\frac{\omega_1}{x}}E_1\left(\bar{a}+\frac{\omega_1}{x}\right)dx,\;\; f_2(a,b)=\int_a^b \frac{\omega_1}{x}e^{-x}E_1\left(\bar{a}+\frac{\omega_1}{x}\right)dx,$$
$$f_3(a,b)=\int_a^b e^{-x+\frac{\omega_1}{x}}E_1\left(\bar{a}+\frac{\omega_1}{x}\right)dx,\;\; f_4(a,b)=\int_a^b e^{-x}E_1\left(\bar{a}+\frac{\omega_1}{x}\right)dx, \tag{41}$$

and

$$\varphi_1^{(1)}=\varphi_1^{(2)}=\varphi_1^{(3)}=\varphi_2^{(1)}=(1-e^{-\bar{a}})^2,\;\; \varphi_3^{(1)}=2(1-e^{-\bar{a}})[1-e^{-\bar{a}}(1+\bar{a})],$$
$$\omega_1=\frac{d_1^m d_2^m \sigma_{n_d}^2\gamma_0}{2\eta P_s},\;\; \theta_0=\frac{\omega_1}{2\bar{a}}. \tag{42}$$

Proof: Please refer to Appendix E. ■

Corollary 4: For the proposed TS-based DF relaying protocol with continuous-time EH, as $\gamma_0 \to 0$, the throughput efficiency can be approximately expressed as

$$\tau \approx \frac{e^{-2\bar{a}}}{2}\frac{\bar{a}+1}{\bar{a}+1+\omega_1} \to \frac{1}{2}. \tag{43}$$

In contrast, as $\gamma_0 \to \infty$, the throughput efficiency obeys the scaling law of

$$\tau \propto \exp(-C_1\gamma_0) \to 0, \tag{44}$$

where C_1 is the same as before.

Proof: Similar to Appendix D, as $\gamma_0 \to 0$, $\breve{I}_0$ becomes the dominant term. Then, it follows from [23, Eq. (5.1.19)] that (40a) reduces to (43). On the other hand, as $\gamma_0 \to \infty$, the three terms ($\breve{I}_0$, $\breve{I}_1$, and $\breve{I}_2$) have to be taken into account to develop the scaling behavior of the throughput efficiency. With the aid of [23, Eqs. (5.1.1) and (5.1.19)], Integration Mean Value Theorem, and after some algebraic arrangements, we can arrive at an expression which scales in proportional to $e^{-2\bar{a}}=\exp(-C_1\gamma_0)$. This completes the proof of Corollary 4. ■

Remark 6:

(i) By comparing Corollaries 3 and 4, we can observe that as $\gamma_0 \to 0$, the proposed adaptive TS factor for DF relaying mode can achieve a higher limiting throughput efficiency (i.e., 0.5) than (37) of the conventional TS factor design. And their performance gap is determined by

the quantity $\frac{d_1^m P_r}{2\eta P_s} e^{\frac{d_1^m P_r}{2\eta P_s}} E_1\left(\frac{d_1^m P_r}{2\eta P_s}\right) \approx \frac{d_1^m P_r}{d_1^m P_r + 2\eta P_s}$. Therefore, for the conventional TS-based DF relaying protocol, we can fill the performance gap by enhancing the energy conversion efficiency η, increasing the transmit power at the source, or by decreasing the first-hop path loss.

(ii) As $\gamma_0 \to \infty$, it follows from Corollaries 3 and 4 that the scaling law (i.e., $e^{-(C_1+C_2)\gamma_0}$) of the conventional TS-based DF relaying protocol is steeper than that of the proposed protocol (i.e., $e^{-C_1\gamma_0}$). In other words, in comparison with the conventional protocol, the throughput efficiency of the proposed one decreases to zero in a much slower pace, a desirable characteristic.

IV. Low-Complexity TS-Factor Design and its Throughput Efficiency

While the proposed TS-based EH relaying protocols in the previous section can achieve remarkable throughput efficiency gains, it requires the instantaneous CSI of both hops to set the TS factor. In order to alleviate the CSI overhead at EH relay while not severely sacrificing the throughput performance, next we present low-complexity TS factor designs for AF and DF modes.

A. AF Relaying

The basic idea is to find an appropriate substitute for the instantaneous CSI of the second hop. It follows from (9) that a direct substitution of $|g_i|^2$ by its mean (unity) does not yield a good performance. This is because when $|g_i|^2$ varies randomly around its mean, the factor $\frac{1}{|g_i|^2}$ changes over a very wide range. Alternatively, we treat $\frac{1}{|g_i|^2}$ as a whole and seek its appropriate substitute. Note that for Rayleigh faded second-hop link, the $|g_i|^2$ conforms to exponential distribution with mean unity, which means that a straightforward replacement of $\frac{1}{|g_i|^2}$ by $E\left[\frac{1}{|g_i|^2}\right]$ is inappropriate since $E\left[\frac{1}{|g_i|^2}\right] = E_1(0) = \infty$. Fortunately, for a sufficiently small positive quantity ε, we have $\Pr\left(|g_i|^2 < \varepsilon\right) = 1 - e^{-\varepsilon} \to 0$. Therefore, we can resort to a sufficiently small positive quantity ε and formulate $\mu \triangleq E\left[\frac{1}{\varepsilon+|g_i|^2}\right] = e^{\varepsilon} E_1(\varepsilon)$ as a substitute for $\frac{1}{|g_i|^2}$. Accordingly, the resultant transmit power at EH relay can be expressed as

$$\tilde{P}_r = \max\left[0, \frac{\mu d_2^m \sigma_{n_d}^2 \gamma_0 (\gamma_{sr,i} + 1)}{\gamma_{sr,i} - \gamma_0}\right]. \tag{45}$$

As in Section II.A, all the energy harvested in the current block will be consumed to boost the throughput efficiency, which yields $\frac{\eta P_s|h_i|^2}{d_1^m}\alpha_i T = \tilde{P}_r\frac{(1-\alpha_i)T}{2}$. Therefore, the TS factor is given by

$$\alpha_i = \frac{d_1^m \tilde{P}_r}{2\eta P_s|h_i|^2 + d_1^m \tilde{P}_r} \triangleq \acute{\alpha}_i. \tag{46}$$

It follows from (46) that the newly harvested energy in the i-th block is $\acute{\alpha}_i T(\eta P_s|h_i|^2/d_1^m)$, while the remaining energy at the end of the i-th block is zero. Notably, the TS factor setting above relies only on the instantaneous CSI of the first hop. As a result, the throughput efficiency of the i-th block can be formulated as

$$\tau_i = \frac{(1-I_{o,i})(1-\acute{\alpha}_i)}{2}, \tag{47}$$

in which $I_{o,i}$ is the same as that in (11). With the aid of (47), next we present the throughput efficiency of the proposed low-complexity TS-factor setting.

Proposition 5: For the low-complexity TS-factor setting in AF relaying mode, the throughput efficiency can be expressed as

$$\tau = \frac{1}{2}e^{-\bar{a}}\int_0^\infty e^{-y}\frac{y+\bar{a}}{\left(\bar{a}+\frac{\mu\gamma_0 d_1^m d_2^m \sigma_{n_d}^2}{2\eta P_s}\right)+y+\frac{\mu d_1^m d_2^m \sigma_{n_d}^2 \bar{a}(1+\gamma_0)}{2\eta P_s y}}dy. \tag{48}$$

In addition, a closed-form approximation to the throughput efficiency can be written as

$$\tau \approx \frac{1}{2}e^{-\bar{a}}\left[1 - B_0 e^{B_0}E_1(B_0)\right], \tag{49}$$

where $B_0 \triangleq \frac{\mu d_1^m d_2^m \sigma_{n_d}^2 \gamma_0}{2\eta P_s}$.

Proof: According to the definition of average throughput efficiency $\tau = E[\tau_i] = \frac{1}{2}E_{|h_i|^2\geq\bar{a}}\left[\frac{1}{1+\frac{B_0}{|h_i|^2-\bar{a}}}\right]$, one can achieve (48) by invoking the change of variables. Then, by following a similar procedure to that in Appendix B.1, one can attain (49). ■

Corollary 5: For the low-complexity TS factor setting in AF relaying mode, as $\gamma_0 \to 0$, the throughput efficiency approaches to 0.5, whereas as $\gamma_0 \to \infty$, the throughput efficiency

approaches to zero with a scaling law of

$$\tau \approx \frac{\eta P_s}{\mu d_1^m d_2^m \sigma_{n_d}^2} \frac{e^{-\bar{a}}}{\gamma_0} \propto \frac{e^{-\bar{a}}}{\gamma_0} \to 0. \tag{50}$$

Proof: Utilizing the tight lower bound given by [23, Eq. (5.1.19)], it follows from (49) that the throughput efficiency can be approximated as $\tau \approx \frac{1}{2}\frac{1}{B_0+1}e^{-\bar{a}}$. Then, as $\gamma_0 \to 0$, we have $\bar{a} \to 0$ and $B_0 \to 0$ such that the throughput efficiency approaches to 0.5. On the other hand, as $\gamma_0 \to \infty$, it is ready to arrive at (50). ■

Remark 7: Based on Corollaries 2 and 5, it can be observed that as $\gamma_0 \to 0$, the proposed low-complexity TS-factor setting can achieve a higher limiting throughput efficiency (i.e., 0.5) than the conventional one. On the other hand, as $\gamma_0 \to \infty$, the throughput efficiency of the conventional TS factor setting is an infinitesimal in comparison with that of the low-complexity TS factor, i.e., $\lim_{\gamma_0 \to \infty} \frac{\sqrt{\frac{\pi}{8}} u^{\frac{1}{2}} e^{-(\sqrt{\bar{a}}+\sqrt{\bar{b}})^2}}{\frac{\eta P_s}{\mu d_1^m d_2^m \sigma_{n_d}^2} \frac{e^{-\bar{a}}}{\gamma_0}} = 0$. In other words, as $\gamma_0 \to \infty$, the throughput efficiency of the low-complexity TS factor setting approaches to zero in a much slower pace than that of the conventional one.

B. DF Relaying

Inspired by the idea in the design of low-complexity TS factor for AF mode, next we present a low-complexity TS-factor design for DF mode. Similar to AF mode, we replace $\frac{1}{|g_i|^2}$ by its statistical approximation $\mu \triangleq E\left[\frac{1}{\varepsilon+|g_i|^2}\right] = e^{\varepsilon} E_1(\varepsilon)$, where ε represents a sufficiently small positive quantity. Accordingly, the transmit power at EH relay can be formulated as

$$\tilde{P}_r = \mu d_2^m \sigma_{n_d}^2 \gamma_0. \tag{51}$$

Interestingly, $\tilde{P}_r$ is now a statistical average irrelevant to the instantaneous CSI. Therefore, the corresponding TS factor α_i can be represented by (19) with $\bar{P}_r$ replaced by $\tilde{P}_r$, i.e., $\alpha_i = \breve{\alpha}_i|_{\bar{P}_r \to \tilde{P}_r}$. Accordingly, the newly harvested energy in the i-th block is $\alpha_i T(\eta P_s |h_i|^2 / d_1^m)$, with α_i given above. While the remaining energy at the end of the i-th block is given by (20), with $\bar{P}_r$ replaced by (51). As thus, the low-complexity TS factor only requires the instantaneous CSI of the first-hop channel. With the aid of Proposition 3, it is ready to attain the throughput efficiency of the

low-complexity TS factor for DF mode, which is summarized in the proposition below.

Proposition 6: For the low-complexity TS factor setting in DF relaying mode, a tight lower bound of the throughput efficiency can be expressed as

$$\tilde{\tau} > \tilde{\tau}^{\mathrm{LB}} = \frac{e^{-\bar{a}-\tilde{b}}}{2}\left(I_0|_{P_r\to\tilde{P}_r} + I_1|_{P_r\to\tilde{P}_r} + I_2|_{P_r\to\tilde{P}_r}\right), \tag{52}$$

where $\tilde{b} \triangleq \frac{\gamma_0 d_2^m \sigma_{n_d}^2}{\tilde{P}_r}$, and I_0, I_1, and I_2 are given by (35a), (35b), and (35c), respectively.

To gain insights of the proposed low-complexity TS factor design, next we characterize the scaling behavior of the throughput efficiency for two extreme cases.

Corollary 6: For the low-complexity TS factor setting in DF relaying mode, the throughput efficiency can be approximated as

$$\tilde{\tau} \approx \frac{e^{-\bar{a}-\tilde{b}}}{2}\left[e^{-\bar{a}} - \frac{d_1^m \tilde{P}_r}{2\eta P_s} e^{\frac{d_1^m \tilde{P}_r}{2\eta P_s}} E_1\left(\bar{a} + \frac{d_1^m \tilde{P}_r}{2\eta P_s}\right)\right] \approx \frac{e^{-2\bar{a}-\frac{1}{\mu}}}{2}\frac{\bar{a}+1}{\bar{a}+1+\frac{\mu d_1^m d_2^m \sigma_{n_d}^2 \gamma_0}{2\eta P_s}}. \tag{53}$$

In particular, as $\gamma_0 \to 0$, the throughput efficiency approaches to 0.5, whereas as $\gamma_0 \to \infty$, the throughput efficiency obeys the scaling law of

$$\tilde{\tau} \propto e^{-C_1\gamma_0} \to 0. \tag{54}$$

Proof: For the low-complexity TS factor setting in DF mode, the first term $\frac{e^{-\bar{a}-\tilde{b}}}{2} I_0|_{P_r\to\tilde{P}_r}$ in (52) is shown to be a tight lower bound and thus we can focus on this quantity to characterize the throughput efficiency. With the aid of (35a) and [23, Eq. (5.1.19)], we can arrive at (53). Then, by jointly considering $\gamma_0 \to 0$ and $\varepsilon \to 0$, it can be confirmed that the limiting throughput efficiency for $\gamma_0 \to 0$ is 0.5. On the other hand, as $\gamma_0 \to \infty$, it follows from (53) that (54) definitely holds, which completes the proof. ■

Remark 8: By comparing Corollary 3 with Corollary 6, we can observe that as $\gamma_0 \to 0$, the low-complexity TS factor can achieve the limiting throughput efficiency of 0.5, which is higher than that of the conventional solution (Corollary 3). As $\gamma_0 \to \infty$, the throughput efficiency of the low-complexity TS factor decays to zero in a much slower pace ($e^{-C_1\gamma_0}$) than that of the conventional one ($e^{-(C_1+C_2)\gamma_0}$).

V. Numerical Results and Discussion

In this section, we first demonstrate the accuracy of the throughput expressions of the proposed EH relaying protocols. Then, we compare the proposed EH relaying protocols with the conventional ones. For comparison purposes and without loss of generality, we adopt the same system parameter setting as in [20]. Unless otherwise specified, we set the transmit power at source to $P_s = 46$ dBm, the energy conversion efficiency to $\eta = 0.5$, the threshold SNR to $\gamma_0 = 60$ dB, the noise variances at the relay and destination nodes to -70 dBm and -100 dBm, respectively. As in [20], the path loss exponent is set to 3, and the distances[8] between source and relay, and between relay and destination are set to 35 and 10 meters, respectively.

In Fig. 1, we show the accuracy of the throughput lower bound for the proposed EH-DF relaying protocol, where we can observe that the proposed analytical lower bound is very tight. Fig. 2 further demonstrates the accuracy of the throughput expression for the proposed EH-AF relaying protocol, as shown in Propositions 1 and 2. From the figure, it can be observed that the exact throughput result matches well with the simulations and the proposed lower and upper bounds are sufficiently tight over the whole threshold SNR regions. In particular, the throughput upper bound as presented in Proposition 2 is tighter than the counterpart in Proposition 1.

Fig. 3 validates the approximated expressions for the throughput efficiency of the conventional as well as the proposed optimal TS factor setting in AF mode, as shown in Corollaries 1 and 2. It can be observed that for the conventional TS factor setting, the approximated expressions are very tight for the threshold SNR regions $\gamma_0 \geq 65$ dB and $\gamma_0 \leq 50$ dB, as stated in Corollary 2. For the proposed (optimal) TS factor setting, the simplified throughput expressions (26a) and (26b) are very tight over the entire threshold SNR regions. Clearly, as $\gamma_0 \to 0$, the proposed optimal TS factor design can achieve a higher limiting throughput efficiency (i.e., 0.5) than the conventional TS factor, which agrees with Corollaries 1 and 2.

[8]With regard to the inter-node distance, the distance setup of 35m and 10m for source-relay and relay-destination links reflects the state of the art for indoor sensor network applications. For example, for the mainstream EH receivers (e.g., P2110/P2110B and P1110 of Powercast), the typical single-hop communications distance ranges from several meters to tens of meters. Then, if the direct link between source (e.g., the power and data transmitter TX91501) and destination (e.g., the access point DM240311, a Microchip 16-bit XLP development board) is blocked by some physical obstacles, we can employ the intermediate sensor node (e.g., WSN-EVAL01) to relay the source's data to the destination.

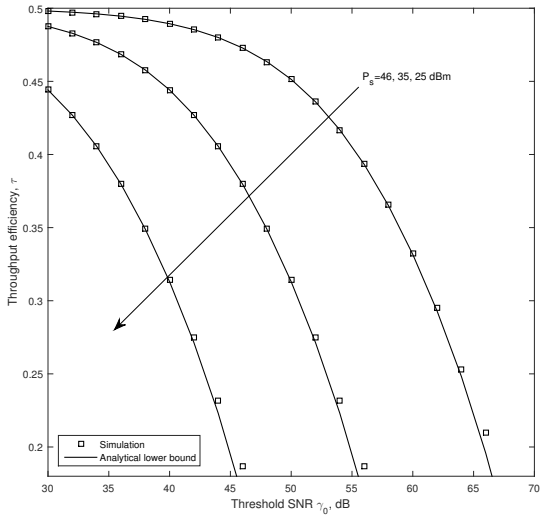

Fig. 1: Throughput efficiency versus the threshold SNR for the proposed EH-DF relaying protocol.

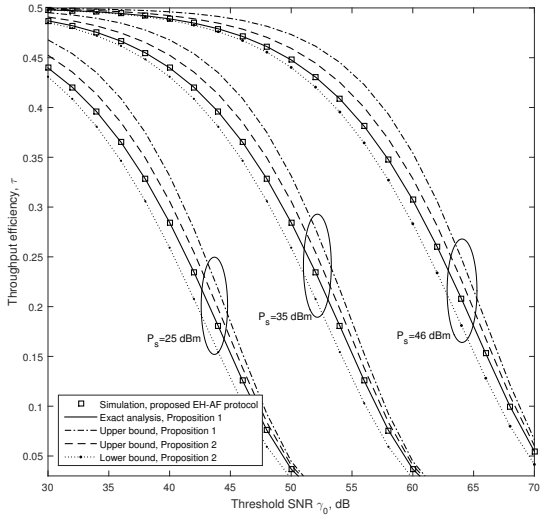

Fig. 2: Throughput efficiency versus the threshold SNR for the proposed EH-AF relaying protocol.

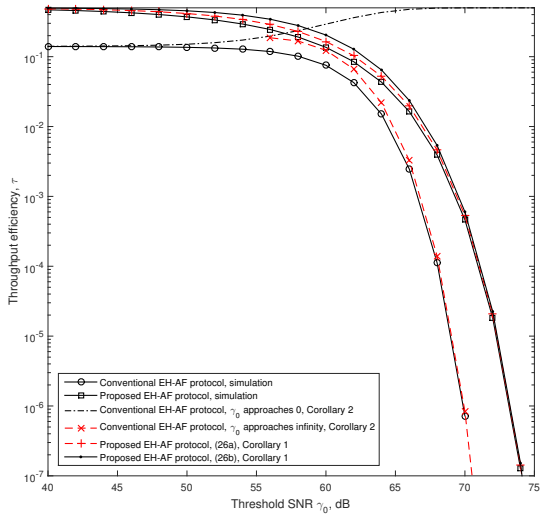

Fig. 3: Throughput efficiency of the conventional and proposed EH-AF protocols for extreme threshold SNR (P_s=35 dBm, d_1=25 m, d_2=10 m).

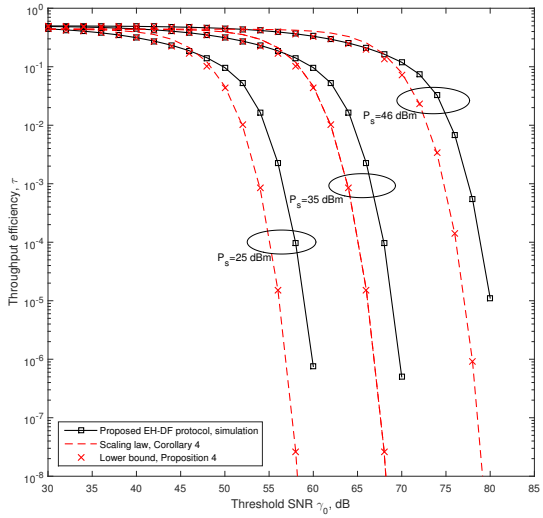

Fig. 4: Throughput efficiency of the proposed EH-DF protocol for extreme threshold SNR.

Fig. 4 plots the throughput efficiency of the proposed optimal TS factor setting in the DF mode. From the figure, we can observe that the scaling law of the throughput efficiency for $\gamma_0 \to \infty$ is valid such that the scaling curves are parallel to the throughput curves for sufficiently high threshold SNR, as predicted in Corollary 4.

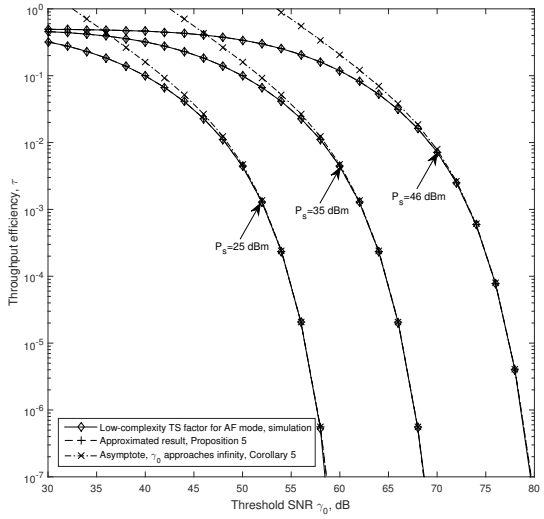

Fig. 5: Throughput efficiency of the proposed low-complexity TS factor setting in AF mode for extreme threshold SNR.

Fig. 5 shows the throughput efficiency of the low-complexity TS factor setting for the AF mode. From the figure, it can be seen that the approximated result presented in Proposition 5 is very accurate over the entire threshold SNR regions. Also, the scaling law presented by Corollary 5 is parallel to the simulated curves in the medium and high threshold SNR regions.

Fig. 6 validates the throughput lower bound in Proposition 6 as well as the approximated throughput efficiency given by Corollary 6. It can be seen that both the lower bound and the approximated results are very tight over the entire threshold SNR regions. In addition, it is clear that the limiting throughput efficiency for $\gamma_0 \to 0$ is 0.5, as predicted by Corollary 6.

Fig. 7 illustrates the energy accumulation process of different TS-based EH relaying protocols for DF mode. It follows from Fig. 7 that with regard to the number of accumulated energy peaks during the first 50 blocks, the proposed optimal TS factor setting contains 4 peaks, the proposed low-complexity TS factor setting contains 5 peaks, whereas the conventional TS factor setting contains 10 peaks. In other words, the proposed optimal/low-complexity TS factor setting can make full use of the harvested energy to transmit information such that excess energy accumulation is avoided, which in turn leads to a superior throughput efficiency.

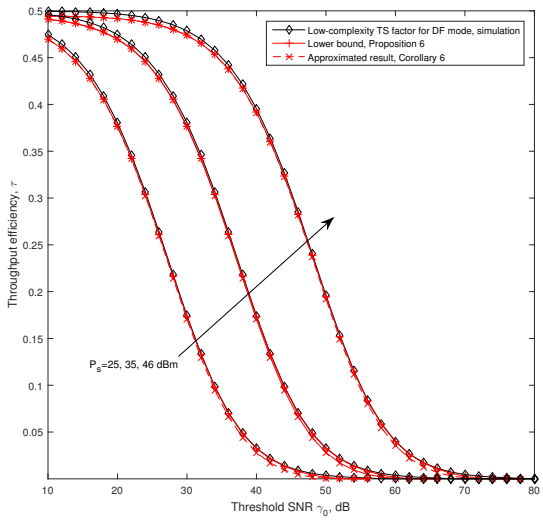

Fig. 6: Throughput efficiency of the proposed low-complexity TS factor setting in DF mode.

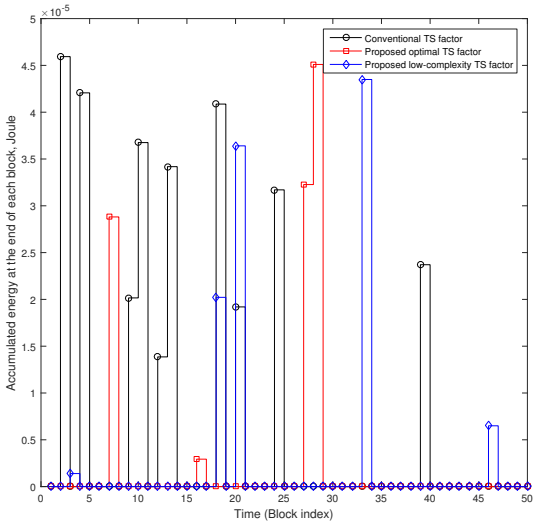

Fig. 7: Energy accumulation process of different TS-based EH relaying protocols in DF mode.

Fig. 8 compares the throughput efficiency of the proposed EH-AF relaying protocol with that of the conventional EH-AF relaying protocol [20]. Herein, the throughput curves of the conventional EH-AF relaying protocol are plotted with the optimal transmit power setting at the EH relay. From the figure, we can observe that the proposed EH-AF protocol outperforms the

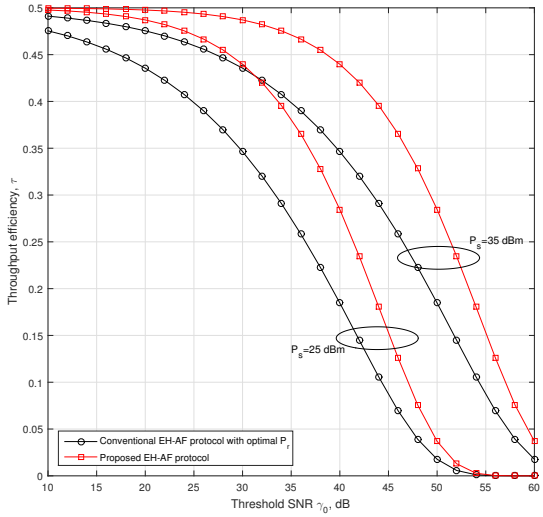

Fig. 8: Comparisons of the proposed EH-AF relaying protocol and the conventional EH-AF relaying protocol with optimal P_r [20].

conventional EH-AF protocol due to the adaptive PS factor and transmit-power setting at the EH relay. Specifically, at $\tau = 0.4$, the proposed protocol can provide more than 8.6 dB threshold SNR gain, whereas at $\tau = 0.3$, the proposed protocol can provide a threshold SNR gain of more than 5.8 dB over the conventional one. In particular, it is noteworthy that for a given throughput efficiency, the threshold SNR gain of the proposed protocol over the conventional one is very stable over a wide transmit power range (i.e., $P_s = 25$ dBm$\sim$35 dBm). Fig. 9 performs a similar analysis of Fig. 8, but assuming EH-DF relaying protocol. The same conclusions hold.

Fig. 10 illustrates the improvement in throughput efficiency (also known as "throughput efficiency gain") of the proposed protocols over the conventional ones. Herein, the optimal transmit power setting is adopted at the EH relay for the conventional protocols. From the figure, we can observe that for a given threshold SNR setup, the throughput efficiency gain in AF mode is very close to the counterpart in DF mode. Also, for both AF and DF modes, the throughput efficiency gain generally increases with the threshold SNR. In addition, with an increase in the transmit power at the source (i.e., P_s), the throughput efficiency gain decreases for both AF and DF modes. This means that a smaller transmit-power at the source leads to a

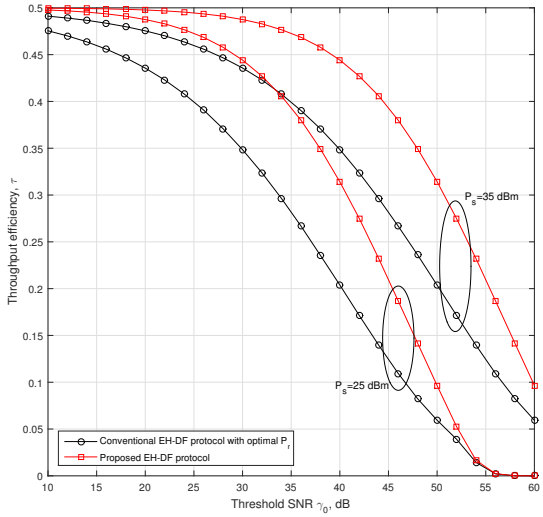

Fig. 9: Comparison of the proposed EH-DF relaying protocol and the conventional one with optimal P_r [20].

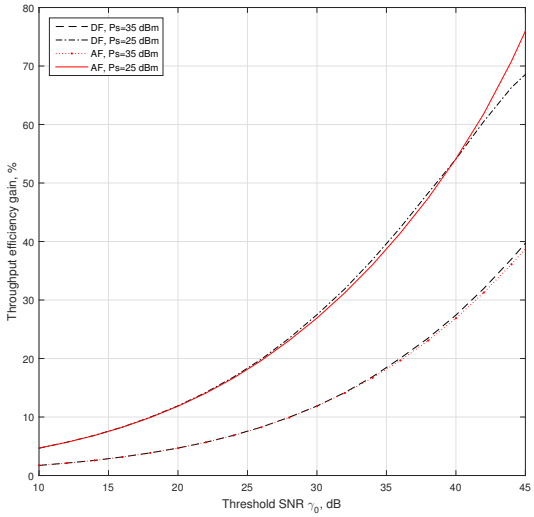

Fig. 10: Throughput efficiency gain of the proposed optimal TS factor setting over conventional one.

larger throughput efficiency gain of the proposed protocols over the conventional ones.

Fig. 11 compares the throughput efficiency of the conventional and the low-complexity TS factor setting for AF relaying mode. From the figure, we can observe that the throughput

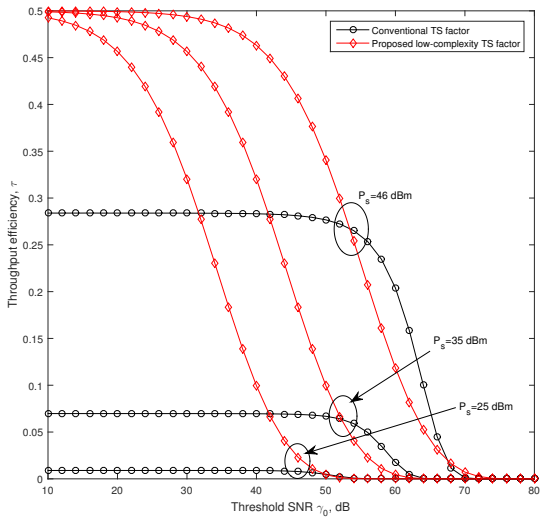

Fig. 11: Comparisons of throughput efficiency between the conventional TS factor and the proposed low-complexity TS factor in AF mode.

efficiency of the low-complexity TS factor setting is superior to that of the conventional TS factor setting especially at low-to-medium threshold SNR region (e.g., $\gamma_0 < 50$ dB). Particularly, for sufficiently small threshold SNR, the low-complexity TS factor setting can always guarantee the limiting throughput efficiency 0.5, as stated by Corollary 5.

Fig. 12 shows the effect of the relay location on the throughput efficiency in AF mode. Herein, we consider a linear network topology and the distances among nodes satisfy to: $d_0 = d_1 + d_2$, with d_0, d_1, and d_2 being the distances between source and destination, between source and relay, and between relay and destination, respectively. It can be seen from the figure that when the EH relay is placed close to the source or close to the destination, the throughput efficiency of the optimal TS factor and the low-complexity ones can be considerably improved. In particular, when the EH relay is close to the source, the throughput efficiency approaches to its limit 0.5, since in this case wireless energy transfer in the first hop tends to be free of path loss. On the other hand, for the conventional TS factor, due to the fixed transmit-power setting at relay, the throughput performance is not good. Particularly, it is shown that when the EH relay is placed around the center between source and destination, a higher P_r is desirable for the conventional

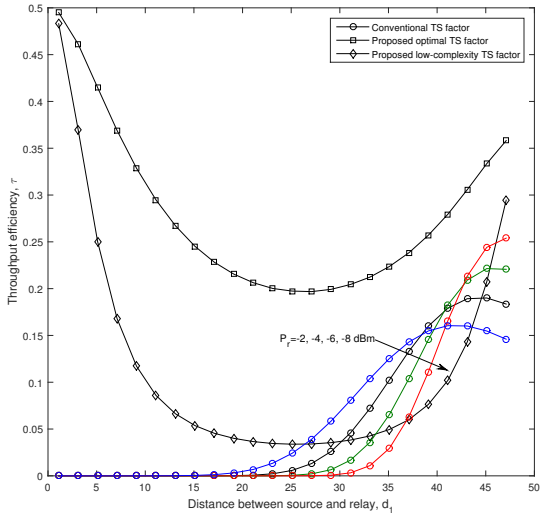

Fig. 12: Throughput efficiency versus the distance between source and relay d_1 in AF mode ($d_0 = 50$ m).

protocol. This is because in this case the path loss between relay and destination is heavy and a larger P_r can avoid the information outage in the second hop, improving therefore the throughput performance. In contrast, when the EH relay is close to destination, the second-hop path loss is light and a smaller P_r is desired for the conventional TS factor setting such that a larger portion of time per block can be used for information transmission to enhance the throughput efficiency.

VI. Concluding Remarks

By making full use of CSI knowledge at EH relay, this paper first proposed an optimal TS factor setting for dual-hop AF (DF) relaying channel, which can achieve the maximum throughput efficiency for each block. To reduce the CSI overhead at EH relay, low-complexity TS factor design was presented for AF and DF modes, which only needs single-hop CSI to determine the TS factor at EH relay. Theoretical results manifested that for sufficiently small threshold SNR, the proposed optimal/low-complexity TS factor setting can achieve a limiting throughput efficiency of 0.5, which is higher than the counterpart of the conventional protocols. In addition, for sufficiently large threshold SNR, the throughput efficiency of the proposed optimal/low-

complexity TS factor approaches to zero in a much slower pace than that of the conventional solutions.

The extension of the proposed TS-based EH relaying protocols to multi-relay scenarios is straightforward. As a whole, the relay selection process can be first implemented to choose one appropriate relay node. And then, the proposed TS-based EH relaying protocols can be carried out. In particular, we can resort to the distributed timer technique to choose relay node in order to lower the implementation complexity [21]. Relying on the CSI knowledge at the candidate relays, we can utilize either dual-hop CSI or the first-hop CSI to perform relay selection in a distributed manner. Specifically, for the proposed optimal TS-factor setting in AF (DF) modes, the best-relay selection scheme can be carried out owing to the dual-hop CSI knowledge at each EH relay [22]. Whereas for the proposed low-complexity TS-factor setting in AF (DF) modes, the partial relay selection scheme can be employed owing to the first-hop CSI knowledge at relays [24].

REFERENCES

[1] L. R. Varshney, "Transporting information and energy simultaneously," *Proc. IEEE Int. Symp. Inf. Theory (ISIT)*, pp. 1612–1616, Jul. 2008, Toronto, Canada.

[2] P. Grover and A. Sahai, "Shannon meets Tesla: Wireless information and power transfer," *in Proc. IEEE Int. Symp. Inf. Theory (ISIT)*, pp. 2363–2367, Jun. 2010, Austin, TX.

[3] X. Zhou, R. Zhang, and C. K. Ho, "Wireless information and power transfer: Architecture design and rate-energy tradeoff," *IEEE Trans. Commun.*, vol. 61, no. 11, pp. 4754–4767, Nov. 2013.

[4] L. Liu, R. Zhang, and K. Chua, "Wireless information transfer with opportunistic energy harvesting," *IEEE Trans. Wireless Commun.*, vol. 12, no. 1, pp. 288–300, Jan. 2013.

[5] P. Popovski, A. M. Fouladgar, and O. Simeone, "Interactive joint transfer of energy and information," *IEEE Trans. Commun.*, vol. 61, no. 5, pp. 2086–2097, May 2013.

[6] L. Liu, R. Zhang, and K. Chua, "Wireless information and power transfer: A dynamic power splitting approach," *IEEE Trans. Commun.*, vol. 61, no. 9, pp. 3990–4001, Sep. 2013.

[7] C. Shen, W.-C. Li, and T.-H. Chang, "Wireless information and energy transfer in multi-antenna interference channel," *IEEE Trans. Signal Process.*, vol. 62, no. 23, pp. 6249–6264, Dec. 2014.

[8] R. Zhang and C. K. Ho, "MIMO broadcasting for simultaneous wireless information and power transfer," *IEEE Trans. Wireless Commun.*, vol. 12, no. 5, pp. 1989–2001, May 2013.

[9] J. Park and B. Clerckx, "Joint wireless information and energy transfer in a two-user MIMO interference channel," *IEEE Trans. Commun.*, vol. 12, no. 8, pp. 4210–4221, Aug. 2013.

[10] A. A. Nasir, X. Zhou, S. Durrani, and R. A. Kennedy, "Relaying protocols for wireless energy harvesting and information processing," *IEEE Trans. Wireless Commun.*, vol. 12, no. 7, pp. 3622–3636, Jul. 2013.

[11] Z. Ding, S. M. Perlaza, I. Esnaola, and H. V. Poor, "Power allocation strategies in energy harvesting wireless cooperative networks," *IEEE Trans. Wireless Commun.*, vol. 13, no. 2, pp. 846–860, Feb. 2014.

[12] I. Krikidis, "Simultaneous information and energy transfer in large-scale networks with/without relaying," *IEEE Trans. Commun.*, vol. 62, no. 3, pp. 900–912, Mar. 2014.

[13] Z. Ding and H. V. Poor, "Cooperative energy harvesting networks with spatially random users," *IEEE Signal Process. Lett.*, vol. 20, no. 12, pp. 1211–1214, Dec. 2013.

[14] I. Krikidis, S. Timotheou, and S. Sasaki, "RF energy transfer for cooperative networks: Data relaying or energy harvesting?" *IEEE Commun. Lett.*, vol. 16, no. 11, pp. 1772–1775, Nov. 2012.

[15] H. Chen, Y. Li, J. L. Rebelatto, B. F. Uchoa-Filho, and B. Vucetic, "Harvest-then-cooperate: Wireless-powered cooperative communications," *IEEE Trans. Signal Process.*, vol. 63, no. 7, pp. 1700–1711, Apr. 2015.

[16] I. Krikidis, "Relay selection in wireless powered cooperative networks with energy storage," *IEEE J. Sel. Area Commun.*, vol. 33, no. 12, pp. 2596–2610, Dec. 2015.

[17] Y. Gu, H. Chen, Y. Li, and B. Vucetic, "Distributed multi-relay selection in accumulate-then-forward energy harvesting relay networks,," Jan. 2016, [Online]. Available:http://arxiv.org/abs/1602.00339.

[18] K. H. Liu, "Performance analysis of relay selection for cooperative relays based on wireless power transfer with finite energy storage," *IEEE Trans. Veh. Technol.*, vol. 65, no. 7, pp. 5110–5121, Jul. 2016.

[19] H. Chen, Y. Li, Y. Jiang, Y. Ma, and B. Vucetic, "Distributed power splitting for SWIPT in relay interference channels using game theory," *IEEE Trans. Wireless Commun.*, vol. 14, no. 1, pp. 410–420, Jan. 2015.

[20] A. A. Nasir, X. Zhou, S. Durrani, and R. A. Kennedy, "Wireless-powered relays in cooperative communications: Time-switching relaying protocols and throughput analysis," *IEEE Trans. Commun.*, vol. 63, no. 5, pp. 1607–1622, May 2015.

[21] A. Bletsas, A. Khisti, D. P. Reed, and A. Lippman, "A simple cooperative diveristy method based on network path selection," *IEEE J. Select. Areas Commun.*, vol. 24, no. 3, pp. 659–672, Mar. 2006.

[22] A. Bletsas, H. Shin, and M. Z. Win, "Cooperative communications with outage-optimal opportunistic relaying," *IEEE Trans. Wirel. Commun.*, vol. 6, no. 9, pp. 3450–3460, Sep. 2007.

[23] M. Abramowitz and I. A. Stegun, *Handbook of Mathematical Functions with Formulas, Graphs, and Mathematical Tables*. New York, 1972.

[24] H. Ding, J. Ge, D. B. da Costa, and Z. Jiang, "Diversity and coding gains of fixed-gain amplify-and-forward with partial relay selection in Nakagami-m fading," *IEEE Commun. Lett.*, vol. 14, no. 8, pp. 734–736, Aug. 2010.

[25] I. S. Gradshteyn and I. M. Ryzhik, *Table of Integrals, Series, and Products*, 7th ed., San Diego, CA: Academic, 2007.

APPENDIX A - PROOF OF PROPOSITION 1

The throughput efficiency of the proposed AF relaying protocol with continuous-time EH can be formulated as

$$\tau = E_{|h_i|^2,|g_i|^2}\{\tau_i\} = \frac{1}{2}E_{|h_i|^2}\left\{E_{|g_i|^2}\left\{(1-I_{o,i})(1-\alpha_i)\right\}\right\} = \frac{1}{2}E_{|h_i|^2\geq\bar{a}}\left\{1-E_{|g_i|^2}\{\alpha_i \mid |h_i|^2\geq\bar{a}\}\right\}. \tag{A-1}$$

With the aid of [25, Eq. (3.352.2)], the term $E_{|g_i|^2}\{\alpha_i \mid |h_i|^2 \geq \bar{a}\}$ in (A-1) can be expressed as

$$E_{|g_i|^2}\{\alpha_i \mid |h_i|^2 \geq \bar{a}\} = \frac{d_1^m d_2^m \sigma_{n_d}^2 \gamma_0(\gamma_{sr,i}+1)}{2\eta P_s |h_i|^2(\gamma_{sr,i}-\gamma_0)} e^{\frac{d_1^m d_2^m \sigma_{n_d}^2 \gamma_0(\gamma_{sr,i}+1)}{2\eta P_s |h_i|^2(\gamma_{sr,i}-\gamma_0)}} E_1\left(\frac{d_1^m d_2^m \sigma_{n_d}^2 \gamma_0(\gamma_{sr,i}+1)}{2\eta P_s |h_i|^2(\gamma_{sr,i}-\gamma_0)}\right), \tag{A-2}$$

where $E_1(\cdot)$ denotes the exponential integral function [23, Eq. (5.1.1)]. Then, by defining $\varpi \triangleq \frac{d_1^m d_2^m \sigma_{n_d}^2 \gamma_0(\gamma_{sr,i}+1)}{2\eta P_s |h_i|^2(\gamma_{sr,i}-\gamma_0)}$ and substituting (A-2) into (A-1), we can arrive at (22) after performing the change of variable and some algebraic arrangements. Making use of the inequality [23, Eq. (5.1.19)], (24) can be achieved, which completes the proof of Proposition 1.

APPENDIX B

B.1 - Proof of Corollary 1:

For AF mode, knowing that $\gamma_{sr,i} = \frac{P_s |h_i|^2}{d_1^m \sigma_{n_r}^2} \gg 1$, we have

$$\frac{d_1^m d_2^m \sigma_{n_d}^2 \gamma_0(\gamma_{sr,i}+1)}{2\eta P_s |h_i|^2(\gamma_{sr,i}-\gamma_0)} \approx \frac{d_1^m d_2^m \sigma_{n_d}^2 \gamma_0 \gamma_{sr,i}}{2\eta P_s |h_i|^2(\gamma_{sr,i}-\gamma_0)} = \frac{C_0}{\gamma_{sr,i}-\gamma_0}, \tag{B-1}$$

where $C_0 = \frac{d_2^m \sigma_{n_d}^2 \gamma_0}{2\eta \sigma_{n_r}^2}$. By plugging (B-1) into (A-2), one can arrive at

$$E_{|g_i|^2}\{\alpha_i \mid |h_i|^2 \geq \bar{a}\} \approx \frac{C_0}{\gamma_{sr,i}-\gamma_0} e^{\frac{C_0}{\gamma_{sr,i}-\gamma_0}} E_1\left(\frac{C_0}{\gamma_{sr,i}-\gamma_0}\right). \tag{B-2}$$

Then, by defining $D_0 \triangleq \frac{d_1^m d_2^m \sigma_{n_d}^2 \gamma_0}{2\eta P_s}$ and using the change of variables, it follows that

$$\tau \approx \frac{1}{2} e^{-\bar{a}} - \frac{1}{2} D_0 e^{-\bar{a}} \int_0^\infty \frac{1}{y} e^{-y+\frac{D_0}{y}} E_1\left(\frac{D_0}{y}\right) dy. \tag{B-3}$$

Next, by using $\frac{1}{x+1} < e^x E_1(x)$ [23, Eq. (5.1.19)], a tight approximation to the throughput efficiency can be expressed as (26a). Then, by invoking $\frac{1}{x+1} < e^x E_1(x)$ again, we can achieve a simple approximation to the throughput efficiency as shown in (26b). After that, by considering $\gamma_0 \to 0$ and $\gamma_0 \to \infty$, we can arrive at the limiting throughput efficiency of 0.5 and (27), respectively. This completes the proof.

B.2 - Proof of Corollary 2:

As stated in [20, Theorem 1], the throughput efficiency for the conventional TS-based AF

relaying protocol with continuous-time EH is given by

$$\tau = \frac{e^{-\frac{a+d}{c}}}{2}\left(uK_1(u) - cd_1^m P_r v\right), \tag{B-4}$$

where $a = P_s d_2^m \sigma_{n_d}^2 \gamma_0$, $b = d_1^m d_2^m \sigma_{n_r}^2 \sigma_{n_d}^2 \gamma_0$, $c = P_s P_r$, $d = P_r d_1^m \sigma_{n_r}^2 \gamma_0$, $u = \sqrt{\frac{4(ad+bc)}{c^2}}$, and $v = \int_0^\infty \frac{e^{-x-\frac{ad+bc}{c^2 x}}}{2c\eta P_s x + 2\eta P_s d + cd_1^m P_r} dx$. As $\gamma_0 \to 0$, it follows from [23, Eq. (9.6.9)] that $uK_1(u) \to 1$. Meanwhile, as $\gamma_0 \to 0$, we have $\frac{a+d}{c} \to 0$. Combining the above results we can arrive at (28). On the other hand, as $\gamma_0 \to \infty$, it can be readily shown that $\lim_{\gamma_0 \to \infty} \frac{cd_1^m P_r v}{uK_1(u)} = 0$. This means that in (B-4), we merely need to preserve $\frac{e^{-\frac{a+d}{c}}}{2} uK_1(u)$ as an effective approximation to (B-4). Then, it follows from [23, Eq. (9.7.2)] that

$$\tau \approx \frac{1}{2} e^{-\frac{a+d}{c}} \sqrt{\frac{\pi u}{2}} e^{-u} \approx \sqrt{\frac{\pi}{8}} u^{\frac{1}{2}} e^{-\left(\sqrt{\bar{a}}+\sqrt{\bar{b}}\right)^2}, \tag{B-5}$$

which completes the proof of Corollary 2.

Appendix C - Proof of Proposition 3

To facilitate the analysis, as in [20, Theorem 3], we make an assumption that $E_o = 0$, which leads to a throughput lower bound of the conventional EH-DF protocol.

To begin with, we consider the case of $n = 0$ (i.e., the number of successive EH blocks due to relay outage is zero). In this case, during the considered EH-IT pattern, no information outage occurs in the first hop prior to the i-th block such that the initial energy of the EH relay at the i-th block is equal to 0, i.e., $E_i(0) = 0$. Otherwise, it follows that $E_i(0) = \eta P_s \sum_{k=1}^{n} |h_{i-k}|^2 T / d_1^m$. Therefore, the TS factor $\tilde{\alpha}_i$ can be expressed as

$$\tilde{\alpha}_i = \begin{cases} 1, \ \text{if } |h_i|^2 < \bar{a}, \\ \frac{d_1^m P_r}{2\eta P_s |h_i|^2 + d_1^m P_r}, \ \text{if } |h_i|^2 \geq \bar{a}, |h_{i-1}|^2 \geq \bar{a}, \\ \frac{d_1^m P_r - 2\eta P_s \sum_{k=1}^{n} |h_{i-k}|^2}{2\eta P_s |h_i|^2 + d_1^m P_r}, \ \text{if } |h_i|^2 \geq \bar{a}, |h_{i-k}|^2 < \bar{a}, \forall k = 1, 2, \ldots, n, |h_{i-(n+1)}|^2 \geq \bar{a}. \end{cases} \tag{C-1}$$

Accordingly, the throughput efficiency of the i-th block can be written as

$$\tilde{\tau}_i = \begin{cases} 0, \ \text{if } |h_i|^2 < \bar{a} \text{ or } |g_i|^2 < \bar{b} \\ \frac{\chi_{0,i}}{2}, \ \text{if } |h_i|^2 \geq \bar{a}, |g_i|^2 \geq \bar{b}, |h_{i-1}|^2 \geq \bar{a} \\ \frac{\chi_{n,i}}{2}, \ \text{if } |h_i|^2 \geq \bar{a}, |g_i|^2 \geq \bar{b}, |h_{i-k}|^2 < \bar{a}, \forall k = 1, 2, \ldots, n, |h_{i-(n+1)}|^2 \geq \bar{a}. \end{cases} \tag{C-2}$$

where $\chi_{0,i} \triangleq 1 - \frac{d_1^m P_r}{2\eta P_s |h_i|^2 + d_1^m P_r}$ and $\chi_{n,i} \triangleq \min\left[1, 1 - \frac{d_1^m P_r - 2\eta P_s \sum_{k=1}^n |h_{i-k}|^2}{2\eta P_s |h_i|^2 + d_1^m P_r}\right]$. By defining $\vec{\mathbf{h}}_n \triangleq \{|h_i|^2, |h_{i-1}|^2, |h_{i-2}|^2, \ldots, |h_{i-n}|^2\}$, the throughput efficiency can be expressed as

$$\begin{aligned} \tilde{\tau} &= E_{|g_i|^2, \vec{\mathbf{h}}_n}\{\tilde{\tau}_i\} = e^{-\bar{b}} E_{\vec{\mathbf{h}}_n}\left\{\tilde{\tau}_i|_{|g_i|^2 \geq \bar{b}}\right\} = e^{-\bar{b}} E_{\vec{\mathbf{h}}_n \setminus |h_i|^2}\left\{\int_{\bar{a}}^{\infty} \tilde{\tau}_i|_{|g_i|^2 \geq \bar{b}, |h_i|^2 \geq \bar{a}} e^{-|h_i|^2} d|h_i|^2\right\} \\ &= \frac{e^{-\bar{b}-\bar{a}}}{2}\Bigg(\underbrace{\int_{\bar{a}}^{\infty} \chi_{0,i} e^{-|h_i|^2} d|h_i|^2}_{I_0} + \underbrace{\int_0^{\bar{a}} \int_{\bar{a}}^{\infty} \chi_{1,i} e^{-|h_i|^2 - |h_{i-1}|^2} d|h_i|^2 d|h_{i-1}|^2}_{I_1} \\ &\quad + \underbrace{\int_0^{\bar{a}} \int_0^{\bar{a}} \int_{\bar{a}}^{\infty} \chi_{2,i} e^{-|h_i|^2 - |h_{i-1}|^2 - |h_{i-2}|^2} d|h_i|^2 d|h_{i-1}|^2 d|h_{i-2}|^2}_{I_2} + \ldots\Bigg) \\ &> \frac{e^{-\bar{b}-\bar{a}}}{2}(I_0 + I_1 + I_2). \end{aligned} \tag{C-3}$$

In what follows, we derive the analytical expressions for I_0, I_1, and I_2. First of all, making use of [25, Eq. (3.352.2)], I_0 can be derived as (35a). Next, turning our attention to I_1, by defining $x \triangleq |h_i|^2$ and $y \triangleq |h_{i-1}|^2$, we have

$$I_1 = \int_0^{\bar{a}} e^{-y} \left(\int_{\bar{a}}^{\infty} \min\left[1, 1 - \frac{d_1^m P_r - 2\eta P_s y}{2\eta P_s x + d_1^m P_r}\right] e^{-x} dx\right) dy. \tag{C-4}$$

For the case $\frac{d_1^m P_r}{2\eta P_s} \leq \bar{a}$, it follows from [25, Eqs. (3.352.2) and (3.351.1)] that

$$I_1 = e^{-\bar{a}}(1 - e^{-\bar{a}}) - \frac{e^{\frac{d_1^m P_r}{2\eta P_s}}}{2\eta P_s} E_1\left(\bar{a} + \frac{d_1^m P_r}{2\eta P_s}\right)\left[d_1^m P_r (1 - e^{-q_1}) - 2\eta P_s (1 - e^{-q_1}(1 + q_1))\right]. \tag{C-5}$$

Similarly, for the case $\frac{d_1^m P_r}{2\eta P_s} > \bar{a}$, it follows from [25, Eqs. (3.352.2) and (3.351.1)] that

$$I_1 = e^{-\bar{a}}(1-e^{-\bar{a}}) - \frac{e^{\frac{d_1^m P_r}{2\eta P_s}}}{2\eta P_s} E_1\left(\bar{a} + \frac{d_1^m P_r}{2\eta P_s}\right)\left[d_1^m P_r(1-e^{-\bar{a}}) - 2\eta P_s(1-e^{-\bar{a}}(1+\bar{a}))\right]. \quad \text{(C-6)}$$

Summarizing (C-5) and (C-6), we can arrive at (35b). Next, we consider the case $n = 2$. By defining $x = |h_i|^2$, $y = |h_{i-1}|^2$, and $z = |h_{i-2}|^2$, we can obtain

$$I_2 = \int_0^{\bar{a}} \int_0^{\bar{a}} \int_{\bar{a}}^{\infty} \min\left[1, 1 - \frac{d_1^m P_r - 2\eta P_s(y+z)}{2\eta P_s x + d_1^m P_r}\right] e^{-x-y-z} dx dy dz. \quad \text{(C-7)}$$

First, we consider the case $0 < \bar{a} \leq \frac{d_1^m P_r}{4\eta P_s}$. Making use of [25, Eqs. (3.352.2) and (3.351.1)], we have

$$I_2 = e^{-\bar{a}}(1-e^{-\bar{a}})^2 - \frac{e^{\frac{d_1^m P_r}{2\eta P_s}}}{2\eta P_s} E_1\left(\bar{a} + \frac{d_1^m P_r}{2\eta P_s}\right)\left[d_1^m P_r(1-e^{-\bar{a}})^2 - 4\eta P_s(1-e^{-\bar{a}}(2+\bar{a}) + e^{-2\bar{a}}(1+\bar{a}))\right], \quad \text{(C-8)}$$

which is equivalent to (35c) for the case $0 < \bar{a} \leq \frac{d_1^m P_r}{4\eta P_s}$. Next, for the case $\frac{d_1^m P_r}{4\eta P_s} < \bar{a} \leq \frac{d_1^m P_r}{2\eta P_s}$, we have to divide the integral region into three areas as bellow

$$\begin{aligned} I_2 = & \iint\limits_{(y,z)\in D_1 \cup D_2} \left(\int_{\bar{a}}^{\infty} \left(1 - \frac{d_1^m P_r - 2\eta P_s(y+z)}{2\eta P_s x + d_1^m P_r}\right) e^{-x} dx\right) e^{-y-z} dy dz \\ & + \iint\limits_{(y,z)\in D_3} \left(\int_{\bar{a}}^{\infty} e^{-x} dx\right) e^{-y-z} dy dz, \end{aligned} \quad \text{(C-9)}$$

where $D_1 = \{0 \leq y \leq y_{P_1}, 0 \leq z \leq \bar{a}\}$, $D_2 = \{y_{P_1} \leq y \leq \bar{a}, y + z \leq 2q_2, z \geq 0\}$, $D_3 = \{y + z \geq 2q_2, y \leq \bar{a}, z \leq \bar{a}\}$, and $y_{P_1} \triangleq 2q_2 - \bar{a}$. Utilizing [25, Eq. (3.352.2)] and after some algebraic manipulations, we can conclude that for $\frac{d_1^m P_r}{4\eta P_s} < \bar{a} \leq \frac{d_1^m P_r}{2\eta P_s}$, (C-9) is equivalent to the first case of (35c). Therefore, summarizing the cases $0 < \bar{a} \leq \frac{d_1^m P_r}{4\eta P_s}$ and $\frac{d_1^m P_r}{4\eta P_s} < \bar{a} \leq \frac{d_1^m P_r}{2\eta P_s}$, we can arrive at the first case of (35c). Now, what remains to be addressed is the case $\bar{a} > \frac{d_1^m P_r}{2\eta P_s}$. For such a case, I_2 can be formulated as

$$I_2 = \left(\iint\limits_{(y,z)\in \tilde{D}_1} + \iint\limits_{(y,z)\in \tilde{D}_2} + \iint\limits_{(y,z)\in \tilde{D}_3}\right) \int_{\bar{a}}^{\infty} \min\left[1, 1 - \frac{d_1^m P_r - 2\eta P_s(y+z)}{2\eta P_s x + d_1^m P_r}\right] e^{-x-y-z} dx dy dz, \quad \text{(C-10)}$$

where $\tilde{D}_1 = \{0 \le y \le \bar{a}, 2q_2 \le z \le \bar{a}\}$, $\tilde{D}_2 = \{2q_2 - z \le y \le \bar{a}, 0 \le z \le 2q_2\}$, and $\tilde{D}_3 = \{0 \le y \le 2q_2 - z, 0 \le z \le 2q_2\}$. Then, by following a similar procedure as before, we can arrive at a closed-form expression of I_2 for the case $\bar{a} > \frac{d_1^m P_r}{2\eta P_s}$, which is shown as the second case of (35c). This completes the proof of Proposition 3.

APPENDIX D - PROOF OF COROLLARY 3

It follows from Appendix C that the term I_0 corresponds to the first type of EH-IT pattern in Section II.B.2, where the EH-IT pattern is composed of a single EH-IT block. As shown by (C-2) and (C-3), this single EH-IT block pattern dominates the throughput efficiency for sufficiently small γ_0. This is because when the received SNR threshold γ_0 is sufficiently small, the relay outage in the first hop becomes a small probability event. As a result, we can resort to the dominant term I_0 to attain tight approximation to the throughput efficiency. As $\gamma_0 \to 0$, we have $\bar{a} \to 0$ and $\bar{b} \to 0$ such that (35a) can be reformulated as

$$I_0 \approx 1 - \frac{d_1^m P_r}{2\eta P_s} e^{\frac{d_1^m P_r}{2\eta P_s}} E_1\left(\frac{d_1^m P_r}{2\eta P_s}\right). \tag{D-1}$$

Then, as $\gamma_0 \to 0$, by ignoring the small probability event I_1 and I_2, we can arrive at (37). On the other hand, as $\gamma_0 \to \infty$, we have $q_1 = \frac{d_1^m P_r}{2\eta P_s}$ and $q_2 = \frac{d_1^m P_r}{4\eta P_s}$ such that φ_1 can be rewritten as

$$\varphi_1 = 1 - 2e^{-\bar{a}} + \left[1 - 2\left(\bar{a} - \frac{d_1^m P_r}{4\eta P_s}\right)\right] e^{-\frac{d_1^m P_r}{2\eta P_s}}. \tag{D-2}$$

Similarly, as $\gamma_0 \to \infty$, φ_2, φ_3, and φ_4 can be written, respectively, as

$$\varphi_2 = 2 + e^{-\bar{a}}(-4 - 2\bar{a}) + e^{-\frac{d_1^m P_r}{2\eta P_s}} \left[2 + \frac{d_1^m P_r}{2\eta P_s} - 2\left(1 + \frac{d_1^m P_r}{2\eta P_s}\right)\left(\bar{a} - \frac{d_1^m P_r}{4\eta P_s}\right)\right], \tag{D-3}$$

$$\varphi_3 = 1 - \left(1 + \frac{d_1^m P_r}{2\eta P_s}\right) e^{-\frac{d_1^m P_r}{2\eta P_s}}, \tag{D-4}$$

$$\varphi_4 = 2 - 2e^{-\frac{d_1^m P_r}{2\eta P_s}} \left(1 + \frac{d_1^m P_r}{2\eta P_s} + \frac{d_1^{2m} P_r^2}{8\eta^2 P_s^2}\right). \tag{D-5}$$

According to the definitions of $\bar{a}$ and $\bar{b}$, we have $\bar{a} \to \infty$ and $\bar{b} \to \infty$ for $\gamma_0 \to \infty$, which by its turn leads to

$$\varphi_1 \approx -2\bar{a}e^{-\frac{d_1^m P_r}{2\eta P_s}}, \tag{D-6}$$

$$\varphi_2 \approx -2\bar{a}\left(1+\frac{d_1^m P_r}{2\eta P_s}\right)e^{-\frac{d_1^m P_r}{2\eta P_s}}. \tag{D-7}$$

Now, by making use of [23, Eq. (5.1.19)], we can attain

$$\begin{aligned} I_1 &\approx e^{-\bar{a}} - \frac{e^{-\bar{a}}}{2\eta P_s\left(1+\bar{a}+\frac{d_1^m P_r}{2\eta P_s}\right)}\left[d_1^m P_r\left(1-e^{-\frac{d_1^m P_r}{2\eta P_s}}\right) - 2\eta P_s\left(1-e^{-\frac{d_1^m P_r}{2\eta P_s}}\left(1+\frac{d_1^m P_r}{2\eta P_s}\right)\right)\right] \\ &\approx e^{-\bar{a}}, \end{aligned} \tag{D-8}$$

where the second approximation holds as $\gamma_0 \to \infty$. By plugging $\varphi_1 \sim \varphi_4$ into I_2 and following a similar procedure as before, as $\gamma_0 \to \infty$, we have $I_2 \approx e^{-\bar{a}}\left[1-\frac{1}{2\eta P_s \bar{a}}\left(d_1^m P_r \varphi_3 - 2\eta P_s \varphi_4\right)\right] \approx e^{-\bar{a}}$. Summarizing the foregoing results, we can achieve an approximated expression of the throughput efficiency for $\gamma_0 \to \infty$ as

$$\tau \approx \frac{3}{2}e^{-2\bar{a}-\bar{b}}, \tag{D-9}$$

which completes the proof of Corollary 3.

APPENDIX E - PROOF OF PROPOSITION 4

To proceed, we make a basic assumption that the available harvested energy at the start of any EH-IT pattern is zero, i.e., $E_o = 0$. This would yield a lower bound for the throughput efficiency. Under this assumption, the TS factor of the i-th block can be written as

$$\hat{\alpha}_i = \begin{cases} \frac{d_1^m \bar{P}_r}{2\eta P_s |h_i|^2 + d_1^m \bar{P}_r}, \ \text{ if } \ |h_i|^2 \geq \bar{a}, |h_{i-1}|^2 \geq \bar{a}, \\ \frac{d_1^m \bar{P}_r - 2\eta P_s \sum_{k=1}^{n} |h_{i-k}|^2}{2\eta P_s |h_i|^2 + d_1^m \bar{P}_r}, \ \text{ if } \ |h_i|^2 \geq \bar{a}, |h_{i-k}|^2 < \bar{a}, \forall k = 1, 2, \ldots, n, |h_{i-(n+1)}|^2 \geq \bar{a}, \\ 1, \ \text{ if } \ |h_i|^2 < \bar{a}, \end{cases} \tag{E-1}$$

in which $\bar{P}_r$ is given by (18). Accordingly, the throughput efficiency of the i-th block can be formulated as

$$\hat{\tau}_i = \begin{cases} \frac{\hat{\chi}_{0,i}}{2}, \ \text{if} \ |h_i|^2 \geq \bar{a}, |h_{i-1}|^2 \geq \bar{a}, \\ \frac{\hat{\chi}_{n,i}}{2}, \ \text{if} \ |h_i|^2 \geq \bar{a}, |h_{i-k}|^2 < \bar{a}, \forall k = 1, 2, \ldots, n, |h_{i-(n+1)}|^2 \geq \bar{a}, \\ 0, \ \text{if} \ |h_i|^2 < \bar{a}, \end{cases} \tag{E-2}$$

in which $\hat{\chi}_{0,i} \triangleq 1 - \frac{d_1^m \bar{P}_r}{2\eta P_s |h_i|^2 + d_1^m \bar{P}_r}$ and $\hat{\chi}_{n,i} \triangleq \min\left[1, 1 - \frac{d_1^m \bar{P}_r - 2\eta P_s \sum_{k=1}^n |h_{i-k}|^2}{2\eta P_s |h_i|^2 + d_1^m \bar{P}_r}\right]$. As a result, a lower bound of the throughput efficiency can be formulated as

$$\begin{aligned} \hat{\tau} &= E_{|g_i|^2, \vec{\mathbf{h}}_n}\{\hat{\tau}_i\} = E_{|g_i|^2, \vec{\mathbf{h}}_n \backslash |h_i|^2}\left\{\int_{\bar{a}}^{\infty} \hat{\tau}_i\big|_{|h_i|^2 \geq \bar{a}} e^{-|h_i|^2} d|h_i|^2\right\} \\ &= E_{|g_i|^2}\left\{\frac{e^{-\bar{a}}}{2}\int_{\bar{a}}^{\infty} \hat{\chi}_{0,i} e^{-|h_i|^2} d|h_i|^2 + \frac{e^{-\bar{a}}}{2}\int_0^{\bar{a}}\int_{\bar{a}}^{\infty} \hat{\chi}_{1,i} e^{-|h_i|^2 - |h_{i-1}|^2} d|h_i|^2 d|h_{i-1}|^2 \right. \\ &\left. + \int_0^{\bar{a}}\int_0^{\bar{a}}\int_{\bar{a}}^{\infty} \frac{e^{-\bar{a}}}{2} \hat{\chi}_{2,i} e^{-|h_i|^2 - |h_{i-1}|^2 - |h_{i-2}|^2} d|h_i|^2 d|h_{i-1}|^2 d|h_{i-2}|^2 + \ldots\right\} \\ &> \frac{e^{-\bar{a}}}{2} E_{|g_i|^2}\left\{I_0\big|_{P_r \to \bar{P}_r} + I_1\big|_{P_r \to \bar{P}_r} + I_2\big|_{P_r \to \bar{P}_r}\right\} \triangleq \hat{\tau}^{\mathrm{LB}}, \end{aligned} \tag{E-3}$$

from which we define $\breve{I}_0 \triangleq E_{|g_i|^2}\left\{I_0\big|_{P_r \to \bar{P}_r}\right\}$, $\breve{I}_1 \triangleq E_{|g_i|^2}\left\{I_1\big|_{P_r \to \bar{P}_r}\right\}$, and $\breve{I}_2 \triangleq E_{|g_i|^2}\left\{I_2\big|_{P_r \to \bar{P}_r}\right\}$. First of all, $\breve{I}_0$ can be readily derived as (40a). Then, we focus on $\breve{I}_1$, which can be expressed as

$$\breve{I}_1 = e^{-\bar{a}}(1 - e^{-\bar{a}}) - \underbrace{E_{|g_i|^2}\left\{\frac{e^{\frac{d_1^m \bar{P}_r}{2\eta P_s}}}{2\eta P_s} E_1\left(\bar{a} + \frac{d_1^m \bar{P}_r}{2\eta P_s}\right)\left[d_1^m \bar{P}_r (1 - e^{-\breve{q}_1}) - 2\eta P_s (1 - e^{-\breve{q}_1}(1 + \breve{q}_1))\right]\right\}}_{\breve{I}_{10}}, \tag{E-4}$$

where $\breve{q}_1 = \min\left[\bar{a}, \frac{d_1^m \bar{P}_r}{2\eta P_s}\right]$. Relying on the value of $\breve{q}_1$, $\breve{I}_{10}$ can be reformulated as

$$\begin{aligned} \breve{I}_{10} &= \int_0^{\frac{\omega_1}{\bar{a}}} e^{-x + \frac{\omega_1}{x}} E_1\left(\bar{a} + \frac{\omega_1}{x}\right)\left[\frac{\omega_1}{x}(1 - e^{-\bar{a}}) - (1 - e^{-\bar{a}}(1 + \bar{a}))\right] dx \\ &+ \int_{\frac{\omega_1}{\bar{a}}}^{\infty} e^{-x + \frac{\omega_1}{x}} E_1\left(\bar{a} + \frac{\omega_1}{x}\right)\left[\frac{\omega_1}{x}(1 - e^{-\frac{\omega_1}{x}}) - \left(1 - e^{-\frac{\omega_1}{x}}\left(1 + \frac{\omega_1}{x}\right)\right)\right] dx. \end{aligned} \tag{E-5}$$

Then, by plugging $\breve{I}_{10}$ into (E-4), one can attain (40b). Next, we turn our attentions to $\breve{I}_2 \triangleq E_{|g_i|^2}\left\{I_2|_{P_r\to\bar{P}_r}\right\}$. To proceed, we have to determine the value of q_2 within $I_2|_{P_r\to\bar{P}_r}$ as below

$$q_2 = \begin{cases} \bar{a}, \ \text{if} \ |g_i|^2 \leq \theta_0, \\ \frac{d_1^m \bar{P}_r}{4\eta P_s}, \ \text{if} \ \theta_0 < |g_i|^2 \leq 2\theta_0, \\ \frac{d_1^m \bar{P}_r}{4\eta P_s}, \ \text{if} \ |g_i|^2 > 2\theta_0, \end{cases} \tag{E-6}$$

which by its turn leads to

$$I_2|_{P_r\to\bar{P}_r} = \begin{cases} e^{-\bar{a}}\varphi_1^{(1)} - \frac{e^{\frac{d_1^m \bar{P}_r}{2\eta P_s}} E_1\left(\bar{a}+\frac{d_1^m \bar{P}_r}{2\eta P_s}\right)}{2\eta P_s}\left(d_1^m \bar{P}_r \varphi_2^{(1)} - 2\eta P_s \varphi_3^{(1)}\right), \ \text{if} \ |g_i|^2 \leq \theta_0, \\ e^{-\bar{a}}\varphi_1^{(2)} - \frac{e^{\frac{d_1^m \bar{P}_r}{2\eta P_s}} E_1\left(\bar{a}+\frac{d_1^m \bar{P}_r}{2\eta P_s}\right)}{2\eta P_s}\left(d_1^m \bar{P}_r \varphi_2^{(2)} - 2\eta P_s \varphi_3^{(2)}\right), \ \text{if} \ \theta_0 < |g_i|^2 \leq 2\theta_0, \\ e^{-\bar{a}}\varphi_1^{(3)} - e^{\frac{2\theta_0\bar{a}}{|g_i|^2}} E_1\left(\bar{a}+\frac{2\theta_0\bar{a}}{|g_i|^2}\right)\left[\frac{2\theta_0\bar{a}}{|g_i|^2}\varphi_2^{(3)} - \varphi_3^{(3)}\right], \ \text{if} \ |g_i|^2 > 2\theta_0, \end{cases} \tag{E-7}$$

in which we have

$$\begin{aligned} &\varphi_1^{(1)} = \varphi_1^{(2)} = \varphi_1^{(3)} = \varphi_2^{(1)} = (1-e^{-\bar{a}})^2, \ \ \varphi_3^{(1)} = 2(1-e^{-\bar{a}})[1-(1+\bar{a})e^{-\bar{a}}] \\ &\varphi_2^{(2)} = 1 - 2e^{-\bar{a}} + \left[1 - 2\left(\bar{a} - \frac{\theta_0\bar{a}}{|g_i|^2}\right)\right] e^{-\frac{2\theta_0\bar{a}}{|g_i|^2}}, \\ &\varphi_3^{(2)} = 2 - 2(2+\bar{a})e^{-\bar{a}} + e^{-\frac{2\theta_0\bar{a}}{|g_i|^2}}\left[2 + \frac{2\theta_0\bar{a}}{|g_i|^2} - 2\left(1+\frac{2\theta_0\bar{a}}{|g_i|^2}\right)\left(\bar{a} - \frac{\theta_0\bar{a}}{|g_i|^2}\right)\right], \\ &\varphi_2^{(3)} = 1 - \left(1 + \frac{2\theta_0\bar{a}}{|g_i|^2}\right) e^{-\frac{2\theta_0\bar{a}}{|g_i|^2}}, \ \ \varphi_3^{(3)} = 2 - 2e^{-\frac{2\theta_0\bar{a}}{|g_i|^2}}\left(1 + \frac{2\theta_0\bar{a}}{|g_i|^2} + \frac{2\theta_0^2\bar{a}^2}{|g_i|^4}\right). \end{aligned} \tag{E-8}$$

As a result, $\breve{I}_2$ can be reformulated as

$$\breve{I}_2 = \int_0^{\theta_0} I_2|_{P_r\to\bar{P}_r} e^{-|g_i|^2} d|g_i|^2 + \int_{\theta_0}^{2\theta_0} I_2|_{P_r\to\bar{P}_r} e^{-|g_i|^2} d|g_i|^2 + \int_{2\theta_0}^{\infty} I_2|_{P_r\to\bar{P}_r} e^{-|g_i|^2} d|g_i|^2. \tag{E-9}$$

By substituting (E-7) into (E-9), we complete the proof of Proposition 4.